

# 1 **Validation of Aura Microwave Limb Sounder stratospheric** 2 **ozone measurements**

3 L. Froidevaux<sup>1</sup>, Y. B. Jiang<sup>1</sup>, A. Lambert<sup>1</sup>, N. J. Livesey<sup>1</sup>, W. G. Read<sup>1</sup>, J. W. Waters<sup>1</sup>,  
4 E. V. Browell<sup>2</sup>, J. W. Hair<sup>2</sup>, M. A. Avery<sup>2</sup>, T. J. McGee<sup>3</sup>, L. W. Twigg<sup>4</sup>,  
5 G. K. Sumnicht<sup>4</sup>, K. W. Jucks<sup>5</sup>, J. J. Margitan<sup>1</sup>, B. Sen<sup>1</sup>, R. A. Stachnik<sup>1</sup>, G. C. Toon<sup>1</sup>,  
6 P. F. Bernath<sup>6,7</sup>, C. D. Boone<sup>7</sup>, K. A. Walker<sup>7,8</sup>, M. J. Filipiak<sup>9</sup>, R. S. Harwood<sup>9</sup>,  
7 R. A. Fuller<sup>1</sup>, G. L. Manney<sup>1,10</sup>, M. J. Schwartz<sup>1</sup>, W. H. Daffer<sup>1</sup>, B. J. Drouin<sup>1</sup>,  
8 R. E. Cofield<sup>1</sup>, D. T. Cuddy<sup>1</sup>, R. F. Jarnot<sup>1</sup>, B. W. Knosp<sup>1</sup>, V. S. Perun<sup>1</sup>, W. V. Snyder<sup>1</sup>,  
9 P. C. Stek<sup>1</sup>, R. P. Thurstans<sup>1</sup>, and P. A. Wagner<sup>1</sup>

10 <sup>1</sup>Jet Propulsion Laboratory, California Institute of Technology, Pasadena, CA, USA.

11 <sup>2</sup>NASA Langley Research Center, USA.

12 <sup>3</sup>NASA Goddard Space Flight Center, USA.

13 <sup>4</sup>Science Systems Applications, Inc. Lanham, MD, USA

14 <sup>5</sup>Harvard-Smithsonian Center for Astrophysics, Cambridge, MA, USA.

15 <sup>6</sup>University of York, York, U.K.

16 <sup>7</sup>University of Waterloo, Waterloo, Ontario, Canada.

17 <sup>8</sup>University of Toronto, Toronto, Canada.

18 <sup>9</sup>University of Edinburgh, Edinburgh, Scotland.

19 <sup>10</sup> Also at New Mexico Institute of Mining and Technology, Socorro, NM, USA.

20  
21  
22  
23 **submitted to JGR (Atmospheres) April 10, 2007**

## 24 25 26 **Abstract**

27  
28 The Earth Observing System (EOS) Microwave Limb Sounder (MLS) aboard the Aura  
29 satellite has provided essentially daily global measurements of ozone (O<sub>3</sub>) profiles from  
30 the upper troposphere to the upper mesosphere since August of 2004. This paper focuses  
31 on validation of the MLS stratospheric standard ozone product (retrieved from the 240  
32 GHz radiometer measurements), with a few results and comments concerning  
33 mesospheric ozone. We use MLS ozone profiles from the recently released version 2.2  
34 data set, in comparisons with correlative ozone profiles taken during the mid-2004 to late  
35 2006 time period. The correlative data are from other satellite instruments, as well as  
36 from aircraft lidar measurements taken during Aura Validation Experiment (AVE)  
37 campaigns and from balloon-borne remote and in situ sensors. We provide a detailed

1 characterization of random and systematic uncertainties for MLS ozone. These estimated  
2 uncertainties and the correlative data comparisons provide the basis for our summary  
3 evaluation of this MLS data product. We typically find better agreement in the  
4 comparisons using MLS version 2.2 ozone than the older version 1.5 data. The  
5 agreement and the MLS uncertainty estimates in the stratosphere are often of order 5%,  
6 with values closer to 10% at the lowest stratospheric altitudes, where small positive MLS  
7 biases can be found. There is very good agreement in the latitudinal distributions  
8 obtained from MLS and from coincident profiles from other satellite instruments, as well  
9 as from aircraft lidar data along the MLS track. The generally excellent agreement with  
10 well calibrated and long-standing correlative ozone measurements in the stratosphere,  
11 together with related validation work comparing MLS ozone profiles versus ground-  
12 based and other aircraft ozone data, establishes the validity of the version 2.2 MLS ozone  
13 data and its uncertainty estimates.

## 14 **1 Introduction**

15 High quality ozone measurements in the current declining phase of stratospheric  
16 chlorine [e.g., *Froidevaux et al.*, 2006b] are essential to better understand the expected  
17 beginning of a slow recovery phase for this important stratospheric gas. Ground-based  
18 and satellite-based measurements of ozone column abundances provide the requisite time  
19 series for assessing expected changes in solar ultraviolet (UV) flux at the ground. Global  
20 ozone profile measurements should enable a more thorough characterization and  
21 understanding of causes and effects (atmospheric forcing and response), including  
22 constraints on atmospheric models and their predictive capabilities. Recently, there has  
23 been a break in the global long-term time series of high quality ozone profile data from

1 the Stratospheric Aerosol and Gas Experiment (SAGE I, SAGE II, and SAGE III) series  
2 of occultation measurements, covering the time period 1979 to 2005, from the Upper  
3 Atmosphere Research Satellite (UARS) Halogen Occultation Experiment (HALOE)  
4 measurements (1991 to 2005), and from the Polar Ozone and Aerosol Measurement  
5 (POAM) experiments (ranging from 1993 to 2005). The 2004 July 14 launch of the Aura  
6 satellite, with four remote sensors on board [*Schoeberl et al.*, 2006a], has led to a new  
7 and extensive data set about the Earth's atmospheric composition. This includes  
8 continuous (day and night) global measurements by the EOS MLS instrument, which  
9 detects thermal emission lines from many trace gases at millimeter to sub-millimeter  
10 wavelengths (see the overview description by *Waters et al.* [2006]); EOS MLS will  
11 mostly be referred to in this work as (simply) MLS, or Aura MLS.

12 In this paper, we present validation results regarding the stratospheric ozone  
13 measurements from MLS, with some comments on the upper (mesospheric) range of  
14 these data. Although MLS measures ozone in several spectral bands, this paper focuses  
15 on the 'MLS standard product' for ozone, retrieved from the MLS radiance  
16 measurements near 240 GHz (radiometer 3, or 'R3'), providing the best overall precision  
17 for the widest vertical range. Version 2.2, the 2<sup>nd</sup> public release of MLS data, has started  
18 "forward processing" since March of 2007, and is currently in the reprocessing stages,  
19 with a much more limited set of days available than version 1.5; 93 days of version 2.20  
20 data are available, covering late 2004 to early 2007, with an emphasis on special months  
21 or days of interest for validation (including campaigns). Comparisons that do not use  
22 MLS data past late 2005, for example, only have about 70 days of reprocessed MLS data  
23 available. Data from version 2.20 (or 02.20) are the validation focus of this paper, since

1 this data version is considered to be the more definitive and improved version. We note  
2 that a subsequent data version, labeled 2.21, includes a minor software patch that affects  
3 the treatment of bad MLS Level 1 radiances, but with essentially no impact, in  
4 comparison to version 2.20, on the days that are reprocessed; the available version 2.20  
5 data can therefore be safely used, and we refer to these and other days (about 2 months  
6 worth at the time of writing) using version 2.21 collectively as version 2.2, or v2.2. The  
7 stratospheric ozone abundance changes between the two versions are found to be quite  
8 systematic in nature, but typically of order 10% or less. Our earlier analyses using v1.5  
9 data [*Froidevaux et al.*, 2006a] demonstrated generally good comparisons (often within 5  
10 to 10%) versus correlative data for January through March 2005. Some perspective with  
11 respect to the original (v1.5) MLS data will be provided in many of the comparisons  
12 discussed here.

13 Section 2 gives a detailed description of the MLS measurements, from (Level 1)  
14 spectral radiances and residuals to (Level 2) retrievals and characterization of  
15 uncertainties. Section 3 provides an array of comparisons between the MLS ozone  
16 profiles and other data sources, from both “routinely-acquired” satellite measurements  
17 and “campaign-related” data sets, geared specifically towards Aura validation. A  
18 companion paper by *Jiang et al.* [2007] provides the results of detailed comparisons  
19 between MLS ozone profiles and ground-based data sets (ozonesondes and lidars).  
20 *Livesey et al.* [2007] provide another MLS companion paper that is coupled to these  
21 analyses of MLS ozone data quality and validation, but focuses on comparisons versus  
22 aircraft measurements of ozone (and carbon monoxide) in the lower altitude region  
23 sampled by MLS (mainly from about 100 to 320 hPa), including the upper troposphere.

1 There are several other recent references that support the assessment of data quality and  
2 the validation of MLS ozone, mainly for the previous data version (v1.5). In particular,  
3 there have been comparisons between MLS ozone and ground-based microwave ozone  
4 profiles from Switzerland [*Hocke et al.*, 2006], and analyses by *Ziemke et al.* [2006] and  
5 *Yang et al.* [2007], focusing on stratospheric columns and resulting tropospheric column  
6 abundances, using a combination of column values from MLS and the Ozone Monitoring  
7 Instrument (OMI), also aboard Aura. In recent work, *Schoeberl et al.* [2007b] use a  
8 trajectory-based analysis and OMI and MLS ozone data, thus leading to a fine horizontal  
9 resolution view of tropospheric ozone residual columns. Comparisons of version 1.5  
10 MLS ozone data with ozone profiles retrieved from 500 GHz observations by the  
11 Submillimetre Radiometer (SMR) aboard the Odin satellite have been described by  
12 *Barret et al.* [2006], who demonstrate typically good agreement (within ~10%) from  
13 about 50 to 0.5 hPa. In this special issue, MLS ozone validation analyses are also  
14 provided by ozone column abundance comparisons between MLS and column  
15 measurements obtained during Aura Validation Experiment (AVE) campaigns by the  
16 Cavity Flux Spectrometer (CAFS) experiment [*Petropavlovskikh et al.*, 2007], as well as  
17 MLS ozone profile comparisons with ground-based microwave radiometer data from  
18 New Zealand and Hawaii [*Boyd et al.*, 2007]. In addition, *Manney et al.* [2007] present a  
19 broad range of comparisons between various MLS data products, including ozone, and  
20 solar occultation data, with a focus on comparisons using equivalent latitude and  
21 potential temperature coordinates.

## 22 **2 MLS Measurements**

23

1       After a brief review of MLS and its measurements (section 2.1), we present typical  
2 Level 1 radiance spectra and residuals in section 2.2. Section 2.3 summarizes the data  
3 usage and screening recommendations for MLS v2.2 ozone profiles, based on analyses of  
4 reprocessed MLS data available at the time of writing, and as used in this work. Sections  
5 2.4 and 2.5 provide a description of estimated MLS ozone uncertainties, both random and  
6 systematic, which we refer to as precision and accuracy. Section 2.6 discusses the  
7 changes from v1.5 to v2.2, both in the retrieval approach and in the average abundances,  
8 as well as the estimated precision and actual scatter in the profiles.

## 9   **2.1 Overview**

10       MLS measures millimeter and submillimeter emission by scanning the Earth's  
11 atmospheric limb every 24.7 s ahead of the Aura satellite, in a sun-synchronous near-  
12 polar orbit with ~1:45 p.m. equatorial crossing time (ascending node), thus providing  
13 retrievals of daytime and nighttime profiles roughly every 165 km along the sub-orbital  
14 track. The instrument uses five broad spectral regions between 118 GHz and 2.5 THz,  
15 covered by seven radiometers. For an overview of the MLS instrument, observational  
16 characteristics, spectral bands, main line frequencies, and target molecules, see *Waters et*  
17 *al.* [2006]. Vertical scans are synchronized to the Aura orbit, leading to retrieved profiles  
18 at the same latitude every orbit, with a spacing of  $1.5^\circ$  great circle angle along the sub-  
19 orbital track; the 240 limb scans per orbit provide close to 3500 profiles per day, stored in  
20 Level 2 data files, in Hierarchical Data Format (more specifically, of the HDF-EOS 5  
21 format type). The vertical retrieval is on a pressure grid with 6 levels (or pressure  
22 surfaces) per decade change in pressure in the stratosphere, and with 3 levels per decade  
23 for pressures smaller than 0.1 hPa. The MLS data from version 1.5 (v1.5) and the recent

1 version 2.2 (v2.2, the focus of this paper) are available from the NASA Goddard  
2 Spaceflight Center Distributed Active Archive Center (DAAC), specifically the Goddard  
3 Earth Sciences (GES) Data and Information Services Center (DISC), at  
4 <http://disc.gsfc.nasa.gov/Aura/MLS/index.shtml>. Public information about MLS and  
5 MLS data access, as well as MLS-related publications, can be found at the MLS website  
6 (<http://mls.jpl.nasa.gov>).

7 The radiometric and spectral performances of the GHz radiometers are discussed by  
8 *Jarnot et al.* [2006]. The MLS retrieval approach is given by *Livesey et al.* [2006] and the  
9 calculation specifics of the MLS radiance model (or ‘forward model’) are described by  
10 *Read et al.* [2006] and *Schwartz et al.* [2006]; line of sight gradients are taken into  
11 account in these retrievals. Section 2.6 provides information on the retrieval changes  
12 that have affected the v2.2 ozone results.

## 13 **2.2 Radiance Spectra and Residuals**

14 The MLS retrievals for the stratospheric and mesospheric components of the ozone  
15 profiles come largely from ozone rotational emission lines measured by band 7 of the R3  
16 radiometer, which also covers CO as a target gas. Calculated spectra for the whole  
17 frequency range (all MLS radiometers) are shown in *Read et al.* [2006], who also provide  
18 sample measured mean spectra and corresponding radiance precisions. Typical radiance  
19 spectra and accompanying residuals (see further below) are shown in Figure 1 for the  
20 aforementioned ozone band. This illustrates typical daily-averaged observed radiances  
21 from the main target ozone line at 235.71 GHz (forming a ‘lower sideband’ contribution  
22 to the microwave signal) and the nearby ozone line at 243.45 GHz (providing an ‘upper  
23 sideband’ contribution); the two sidebands of this detected signal are combined into the

1 measured ‘double-sideband’ radiances. The line wing component of emission arising  
2 from the 244.16 GHz ozone line (in the upper sideband) is also evident in the spectra of  
3 Figure 1, which shows radiances arising from various tangent heights, from the upper  
4 troposphere (near 10 km) to the upper stratosphere (near 50 km), where the lines are  
5 much narrower; the band 7 mesospheric retrievals rely mainly on the narrow digital  
6 autocorrelator spectrometer (DACS) channels near the ozone line center. The residuals  
7 shown in Figure 1 are obtained by differencing the calculated (forward model) average  
8 radiances from the measured average radiances arising from one day of atmospheric  
9 profiles (trace gases and temperature) retrieved by the MLS v2.2 algorithms. The same  
10 patterns (for average radiances and residuals) are evident if we use the same day, but a  
11 year apart (not shown here). The typical average residuals obtained from Fig. 1 are of  
12 order a few tenths of 1K to slightly above 1K. This compares to signal strengths (spectral  
13 contrast above the baseline being important here) of order 50-100K, so the residual errors  
14 are of order 1%. Such good ozone retrieval closure is typically obtained by the MLS  
15 algorithms, with remaining small radiance differences expected to contribute only in a  
16 small way to errors in the retrieved product. Based on radiance noise of order 1 to 4 K  
17 for individual measurements from this band [see *Waters et al.*, 2006], the expected  
18 precision for daily-averages (with more than 3000 spectra per day at each height) is less  
19 than 0.1K. There is therefore a small but systematic component in these residuals  
20 (typical of other days’ results, not shown here), and removing or further reducing such  
21 systematics is a desired task for a future MLS retrieval version.

22 A pressure/latitude contour plot of typical daily zonal mean “chi square” values for the  
23 ozone band (band 7) is shown in Figure 2 (top panel); these values provide an average

1 representation of the sum of the squared radiance residuals divided by the square of the  
2 estimated radiance errors for each tangent viewing location. The median values (not  
3 shown) are typically between 1 and 2, but the average values are affected by a limited  
4 number of larger values representing poorer fits and/or fewer radiances, especially in the  
5 upper troposphere and at tropical latitudes. Figure 2 (bottom panel) shows a related plot  
6 versus latitude for the “Quality” field, stored in the MLS Level 2 ozone files. “Quality”  
7 gives a simple (one number per profile) measure of radiance fits based on the overall chi  
8 square value, and is directly related to the combination of radiance chi square values for  
9 each profile. This plot shows that minima in quality (the poorest quality profiles) occur  
10 in the latitudinal regions where the highest zonal mean values of chi square occur, with  
11 largest chi square values typically occurring at the lowest altitudes (upper troposphere).  
12 As done for v1.5 data [*Livesey et al.*, 2005], we recommend (see next section) a  
13 “Quality” threshold for data screening.

### 14 **2.3 Data Usage and Screening**

15 The recommendations below for screening the stratospheric (and mesospheric) MLS  
16 ozone profiles (standard product) are similar to those given for version 1.5 data (see  
17 *Livesey et al.* [2005]). However, there are slightly different threshold values for v2.2,  
18 because of some rescaling of the relationship between radiance fits and the “Quality”  
19 flag, and there is also a new flag (“Convergence”) to take into account.

20 **Status Field:** As for v1.5 data, ozone profiles should be used if the field named “Status”  
21 (found in the ozone Level 2 files) has an even value; this field will have an odd value if  
22 the retrieval diverged or not enough radiances were used, or some other anomalous  
23 instrument or retrieval behavior occurred. The retrieved profile may be considered

1 “questionable” if “Status” is non-zero, for example if clouds may have affected some of  
 2 the radiances used for each set (or “chunk”) of retrieved profiles; these chunks typically  
 3 include 10 or 11 profiles, see *Livesey et al.* [2006]. However, we have found no evidence  
 4 to recommend an outright rejection of all profiles with such “questionable” Status values,  
 5 when inspecting how these profiles compare to other profiles at similar latitudes, and we  
 6 note that the questionable radiances have not been used in these ozone retrievals. Table 1  
 7 summarizes the various bit values that can be set and affect the value of “Status”.

8

9 **Table 1.** Meaning of bits in the “Status” field.

10

| Bit | Value <sup>a</sup> | Meaning                                                                                       |
|-----|--------------------|-----------------------------------------------------------------------------------------------|
| 0   | 1                  | Flag: Do not use this profile (see bits 8-9 for details)                                      |
| 1   | 2                  | Flag: This profile is ‘suspect’ (see bits 4-6 for details)                                    |
| 2   | 4                  | Unused                                                                                        |
| 3   | 8                  | Unused                                                                                        |
| 4   | 16                 | Information: This profile may have been affected by high altitude clouds                      |
| 5   | 32                 | Information: This profile may have been affected by low altitude clouds                       |
| 6   | 64                 | Information: This profile did not use GEOS-5 temperature a priori data                        |
| 7   | 128                | Unused                                                                                        |
| 8   | 256                | Information: Retrieval diverged or too few radiances available for retrieval                  |
| 9   | 512                | Information: The task retrieving data for this profile crashed (typically a computer failure) |

11

12 <sup>a</sup>“Status” field in L2GP file is total of appropriate entries in this column.

13

14 **Quality Field:** As mentioned in the previous section, the Quality field in the Level 2  
 15 ozone files can discriminate retrieved profiles that have poor radiance fits, although no  
 16 specific information is provided about which height(s) exhibit the worst fit, unless one  
 17 inspects the MLS Level 2 “DGG” files in more detail to examine the height-dependence  
 18 of radiance chi square values. The poorest fits exist at the lowest altitudes and often in  
 19 the tropics; this might be in relation to cloud-related effects on the MLS radiances. We

1 recommend use of stratospheric ozone profiles with Quality > 0.4, in order to screen out  
2 the poorest radiance fits (1% or less, typically, of available daily profiles). We note that a  
3 tighter criterion (Quality > 1.2) is recommended for the upper troposphere [*Livesey et al.*,  
4 2007], meaning primarily for low latitude regions at pressures of 100 hPa or more.

5 **Convergence Field:** This is a new (version 2.2) field in the L2GP files, and it refers to  
6 the ratio of chi square value, from radiance fits for each “chunk” of typically ten profiles,  
7 to the value that the retrieval would have been expected to reach. Since we have not  
8 generally observed anomalous behaviors for the profiles with larger than average values  
9 of Convergence, a field with values between 1 and 1.1 for the vast majority of profiles,  
10 we recommend use of ozone profiles with Convergence < 1.8. This eliminates a very  
11 small fraction of the available ozone profiles, as many days do not have any such  
12 profiles; on occasion, a few profile chunks get flagged by such a Convergence value.

13 **Precision values:** As done before for v1.5 data, we recommend that users ignore the  
14 ozone profiles at pressures where the estimated precision values are flagged negative; at  
15 these pressures (typically only for 0.01 hPa and lower pressures), the influence of the  
16 a priori profile becomes large (estimated precision divided by a priori error becomes less  
17 than 0.5). The pressures (in the mesosphere and troposphere) where the precision values  
18 do provide a data screening criterion generally occur at a fairly sharp transition between  
19 good and poor MLS sensitivity, although there is still some MLS sensitivity in the  
20 uppermost mesosphere, for example, if one were to use average abundances.

21 **Vertical Range:** Our analyses of MLS sensitivity and precision, coupled with the  
22 characterization and validation studies described here and in the related upper  
23 tropospheric analyses [*Livesey et al.*, 2007], lead us to recommend that only MLS ozone

1 values at pressures from 215 to 0.02 hPa be used. The 147 and 215 hPa MLS retrieval  
2 grid levels generally lie in the upper troposphere at low latitudes, but can be in the  
3 stratosphere at high latitudes. The limit at 0.02 hPa is a conservative single-profile  
4 sensitivity limit, although studies of ozone at higher altitudes may be performed, with  
5 caution (and preferably in consultation with the MLS team).

6 In summary,

7 *data users should only use MLS ozone profiles from 215 to 0.02 hPa with*

- 8 ● even value of Status and
- 9 ● positive precision values and
- 10 ● Quality value  $> 0.4$  (with a higher cutoff value of 1.2 for 100 to 215 hPa)
- 11 ● Convergence value  $< 1.8$

12 We feel that these criteria will generally allow for the reliable use of more than roughly  
13 97% of the available daily MLS ozone profiles, with the precision and accuracy described  
14 later in this work being applicable.

## 15 **2.4 Precision and Resolution**

16 The precision and resolution of the retrieved MLS ozone profiles limit the degree to  
17 which comparisons with other ozone profiles should agree, and the analysis and  
18 interpretation of such comparisons. The MLS antenna field of view for the 240 GHz  
19 radiometer (relevant for the ozone product discussed here) has a width of 3.2 km at the  
20 limb tangent point in the vertical direction, and 6.4 km in the horizontal (across-track)  
21 direction [Waters *et al.*, 2006]. The measurement resolution is also affected by the  
22 radiative transfer averaging path through the atmosphere. The resolution, both vertical

1 and along the MLS sub-orbital track, can be visualized through the use of the averaging  
2 kernel matrix, as described for atmospheric retrievals by *Rodgers* [1976]. Figure 3  
3 displays vertical and horizontal averaging kernels for a typical MLS ozone retrieval. This  
4 figure also depicts (as thick dashed black lines) the corresponding vertical and horizontal  
5 resolution of the ozone profiles, using the half width at full maximum of the averaging  
6 kernels as such a measure. The integrated value of the averaging kernels is generally  
7 very close to unity in the region where the influence of a priori profile information on the  
8 retrievals is negligible. For ozone, we see that this condition is satisfied for the range  
9 from 316 to 0.01 hPa. The inferred vertical resolution is about 2.7 to 3 km for a large  
10 part of the recommended retrieval range, from the upper troposphere to the mesosphere.  
11 We have generated such averaging kernel plots for various latitudes and the changes for  
12 different conditions are quite small. The triangular and well-peaked nature of the  
13 averaging kernels for these limb sounding measurements is a desirable characteristic,  
14 although there are resolution limitations to keep in mind.

15 The precision of the ozone measurements can be arrived at from the uncertainties that  
16 are estimated by the MLS retrieval calculations, following the general *Rodgers* [1976]  
17 formulation, see *Livesey et al.* [2006]; these uncertainty estimates are provided in the  
18 MLS Level 2 files (for each profile), as the diagonal values of the error covariance  
19 matrix. Figure 4 shows typical values of this estimated precision, along with an empirical  
20 estimate from root mean square (rms) scatter about the mean for matched profile pairs  
21 from the ascending and descending portions of the orbit. Note that this scatter has been  
22 reduced by square root of two in the plot shown here, since the scatter between ascending  
23 and descending MLS profiles should be larger, by this factor, than the individual

1 precision. The coincidence criterion chosen here, for the maximum distance separating  
2 the ascending and descending profiles, is 300 km. This scatter for ascending and  
3 descending profiles is quite similar to the rms scatter within a narrow latitude bin where  
4 atmospheric variability is expected to be small (such as for 5°S to 5°N in the middle  
5 stratosphere). The precision obtained from the scatter in (ascending versus descending)  
6 MLS profiles is generally larger than the estimated precision in the stratosphere and  
7 upper troposphere, as atmospheric variability adds some scatter. The scatter is also  
8 sometimes somewhat less than the estimated precision, as can be observed for the  
9 mesosphere; this is a result of the retrieval a priori influence and smoothing constraints,  
10 even though there is no smoothing constraint for pressures less than 0.1 hPa. The mean  
11 differences between the ascending and descending profiles (shown as dots in Figure 4)  
12 are typically very small in the stratosphere, but there are significant differences in the  
13 upper stratosphere and mesosphere, due to diurnal variation at these heights.

14 Figure 5 shows a contour plot of the estimated root mean square (rms) precision for  
15 latitudinally-binned MLS ozone retrievals on a typical day, for 24 September, 2004. The  
16 precision values (as obtained from the Level 2 data files) can be as low as 30 ppbv from  
17 100 to 215 hPa, and increase to 0.3 ppmv near 1 hPa. Although the precision is fairly  
18 constant versus latitude, there can be variations of a factor of two, especially at the lower  
19 altitudes, between equatorial and polar regions.

#### 20 ***MLS Column Abundance Precision***

21 The expected precision in MLS column abundances down to pressures of 100 to 215 hPa  
22 is about 2 to 4 Dobson Units (DU), or 2%, based on an analysis of simulated retrievals.  
23 Comparisons of actual MLS measurements from ascending and descending sides of the

1 orbits, and variability in tropical measurements, lead to 3% as a conservative estimate for  
2 the MLS column ozone precision.

### 3 **2.5 Expected Accuracy**

4 As part of the validation process, we want to characterize the systematic  
5 uncertainties of the retrieved profiles. Comparisons with well-characterized and accurate  
6 data can provide valuable information (see section 3), and so can an assessment of known  
7 or potential error sources. Systematic errors arise from instrumental effects such as  
8 imperfect radiometric calibration or field of view characterization, as well as from errors  
9 in laboratory spectroscopic data, or retrieval formulation and implementation. This  
10 section summarizes our quantification of these errors for ozone. Details of this  
11 assessment approach are given in the Appendix of *Read et al.* [2007].

12 For each source of systematic error, the impact on the MLS radiance measurements  
13 (or pointing, where appropriate) has been quantified and modeled. These modeled effects  
14 correspond to either 2 sigma estimates of uncertainty in the modeled quantity, instrument  
15 calibration uncertainty, or the sensitivity to a priori. The impact of these perturbations on  
16 retrieved MLS products has been quantified for each error source by one of two methods.  
17 In the first method, modeled errors have been applied to simulated MLS radiances, based  
18 on a model atmosphere, for a whole day of MLS observations. These perturbed radiances  
19 have then been run through the routine MLS data processing algorithms, and the  
20 systematic errors have been evaluated from the impact of the perturbation on the Level 2  
21 products (i.e., the resulting differences from an “unperturbed” run). In addition to giving  
22 an estimate of any bias introduced by the various error sources, these “full up” studies  
23 also quantify any additional scatter (standard deviation about the mean bias) introduced

1 in the retrievals by each error source. The difference between the retrieved product in the  
2 unperturbed run and the original “true” model atmosphere is taken as a measure of errors  
3 due to retrieval formulation and numerics. The impact of some remaining (typically  
4 small) systematic errors has been quantified through analytic calculation based on  
5 simplified models of the MLS measurement system [Read *et al.*, 2007]. Figure 6  
6 provides a summary of these error analyses for ozone.

7 The results shown in Figure 6 point to possible biases of about 0.05 to 0.3 ppmv for  
8 most of the stratosphere (100 to 1 hPa), with total errors (including the random  
9 component) of about 5 to 10% in this region. The bias (typically under 7% in this region)  
10 is the error one might expect to see in a multi-profile comparison versus “true” profiles,  
11 whereas the total uncertainty is more relevant for single profile comparisons, as it  
12 includes a random component (scatter). Accuracy estimates have also been looked at in  
13 terms of multiplicative terms and additive biases, as discussed for the lower altitude  
14 region by Livesey *et al.* [2007]. The estimated (percent) uncertainties increase at higher  
15 pressures, as the ozone values can become small in the tropics and upper troposphere.  
16 Values for the estimated uncertainties at selected pressures are tabulated in the last  
17 section of this paper (see Table 2), as a summary of the results of Figure 6 and other  
18 relevant analyses in this paper.

19 Especially in the lower stratosphere, the ozone uncertainties estimated here are  
20 significantly smaller (better) than those of UARS MLS, estimated at ~0.3 ppmv [see  
21 Froidevaux *et al.*, 1996], primarily due to the wider bandwidth of the Aura MLS  
22 spectrometers. Results in Figure 6 and from other analyses (not shown) of the individual  
23 components contributing to each of these families of curves [Read *et al.*, 2007] show that

1 the major contributors to the ozone uncertainty are from (a) pointing-related uncertainties  
2 (red curves), (b) radiometric and spectral calibration (cyan curves), and (c) retrieval  
3 formulation (grey curves). Ozone spectroscopic error contributions, the largest  
4 component of the values shown by the green curves, are not a major fraction of the total  
5 errors, which means that large improvements in the ozone accuracy are not expected from  
6 better spectroscopic knowledge of the linewidth for the 240 GHz emission lines (this  
7 linewidth is estimated to be known at the 3% level); the oxygen line width uncertainty  
8 (also 3%, see *Read et al.* [2007]) contributes to pointing uncertainty as well, but only as  
9 roughly one third of the total. Finally, we note that cloud-related errors (purple curves)  
10 do not contribute much to the total error; this adds confidence to our recommendation not  
11 to discard MLS ozone profiles that may be in the vicinity of clouds, as determined by  
12 MLS “window channel” radiances [*Wu et al.*, 2007] and the related MLS ozone “Status”  
13 values.

#### 14 ***Biases between MLS Ozone Bands***

15 Figure 7 compares the average profiles (versus latitude) from separate retrievals  
16 using the various MLS ozone bands. The differences shown in this figure are based on  
17 February and March 2005 averages (using 32 days of available MLS v2.2 data), and are  
18 typical of the differences observed on other days. Differences are typically between plus  
19 or minus 3 to 9% in the middle stratosphere, consistent with accuracies on each ozone  
20 product of about 5 to 7%; we do know that the non-standard MLS ozone products are  
21 generally not in as good an agreement versus correlative data as the MLS standard ozone  
22 product. This illustrates that systematic differences in retrievals of the same atmospheric  
23 gas from different frequencies can certainly exist, even from the same instrument. This

1 result and the earlier analyses underlie the fact that an accuracy for MLS ozone of better  
2 than a few to 5% is difficult to attain (and also difficult to prove from comparisons).

### 3 ***MLS Column Abundance Accuracy***

4 The expected accuracy in the column abundances, using MLS ozone profile  
5 integrations down to pressures of 100 to 215 hPa, has also been assessed from the  
6 sensitivity analyses mentioned above. We find that the (2 sigma) accuracy estimate for  
7 columns arising from the integration of MLS ozone profiles down to pressure levels of  
8 100 to 215 hPa is about 4%.

## 9 **2.6 Differences between v2.2 and v1.5 Data**

10

11 We now discuss why there are differences between the v1.5 and v2.2 ozone products  
12 from MLS, and provide a sense of the magnitude and characteristics of these changes.  
13 Version 2.2 differs from version 1.5 mainly because of indirect effects from the coupled  
14 retrievals of temperature and tangent pressure, as discussed by *Schwartz et al.* [2007].  
15 The use of slightly different bands and channels, as well as some calibration corrections  
16 for the digital autocorrelator spectrometer (DACS) channels used in these retrievals, have  
17 led to slightly lower values for the MLS temperatures, and a related shift in tangent  
18 pressure, increasing from near zero in the lower stratosphere to the equivalent of a few  
19 hundred meters near 1 hPa. Also, a finer retrieval grid is used for temperature (and H<sub>2</sub>O)  
20 for pressures larger than 20 hPa, although this is not the main reason for the changes.  
21 Mesospheric changes have also occurred as a result of the calibration changes for the  
22 DACS channels used in the center of band 7, for the standard (240 GHz) MLS ozone  
23 product.

1 The changes observed in MLS ozone are systematic in nature, and there is not much  
2 change in the scatter or precision of stratospheric or mesospheric ozone data. Figure 8 is  
3 a pressure/latitude contour plot of the average differences observed between the two MLS  
4 data versions (v2.2 minus v1.5), expressed as a percentage of the v1.5 zonal means, using  
5 the combination of available reprocessed v2.2 (and v1.5) days, ranging from September  
6 2004 to October 2006. The changes are relatively constant as a function of latitude;  
7 slightly lower abundances are retrieved near 100 hPa, near-zero change occurs at about  
8 15-20 hPa, as well as near 0.5 hPa, while larger abundances (by about 10%) are now  
9 observed near 1 hPa. The mesospheric values are now typically lower, with larger  
10 departures from v1.5 as height increases, changes of -10% to -30% in the upper  
11 mesosphere. The average differences depicted in Figure 8 are characteristic of the zonal  
12 mean changes on any given day. Figure 9 shows global mean differences between v2.2  
13 and v1.5 data over available v2.2 days from late 2004 to late 2006, at a few selected  
14 pressures. Although the changes are fairly invariant as a function of time, there can be  
15 variations in these differences of order a few percent, depending on pressure. Other plots  
16 (not shown here) indicate that the seasonal or year-to-year changes at various latitudes  
17 are overall very similar for both data versions.

### 18 ***Column Abundance Differences***

19 We note that the changes mentioned above for MLS profiles have led to a slight  
20 reduction in stratospheric column abundances that can be calculated from an integration  
21 of the profiles above the tropopause, or in column abundances down to pressures larger  
22 than (or equal to) 100 hPa. As mentioned by *Yang et al.* [2007], some compensation  
23 occurs from higher altitudes, where the MLS ozone profile values have increased

1 somewhat, but the decrease in MLS ozone abundances in the lower stratosphere and  
2 upper troposphere drive the slight reduction in stratospheric ozone columns. Depending  
3 on the lower pressure level used for column integration (from 100 to 215 hPa), we find  
4 that the MLS column decreases are ~0.5 to 2% between the two data versions, with a  
5 standard deviation of 4 to 5%. The average differences typically amount to a few DU.

### 6 **3 Comparisons with other data sources**

7  
8 We now compare MLS v2.2 ozone profiles with various data sets; v1.5 comparisons  
9 are often included to show the changes.

#### 10 **3.1 Comparisons with satellite data**

##### 11 *MLS and SAGE II Profiles*

12 The SAGE II ozone profiles, measured via solar occultation at wavelengths near  
13 600 nm, with a vertical resolution of about 1 km, have been validated extensively  
14 [H.-J. Wang *et al.*, 2002; P.-H. Wang *et al.*, 2006] and have provided one of the best  
15 available data sources (in combination with SAGE I data) for studying long-term trends  
16 in ozone profiles [e.g., WMO, 2003]. We should therefore be able to rely on comparisons  
17 with SAGE II to ascertain the quality of MLS stratospheric ozone profiles. Comparisons  
18 with SAGE III are not shown here, but the analyses by H.-J. Wang *et al.* [2006] have  
19 shown that the SAGE III ozone results do not differ much from SAGE II, with SAGE III  
20 typically giving larger values by a few to 5 percent. The SAGE III data set is also more  
21 limited in latitude, as the orbital characteristics of the SAGE III instrument were chosen  
22 to focus on the high latitudes. Good agreement between v1.5 MLS and SAGE III ozone

1 profiles has been presented by *Yang et al.* [2007], and by *Manney et al.* [2007], for MLS  
2 v2.2 data.

3 We first use about 2 months of (non-contiguous) days of MLS v2.2 data to illustrate  
4 the effects of interpolation and smoothing methods on the comparisons. Figure 10  
5 provides the average percent differences between MLS v2.2 and coincident SAGE II  
6 (version 6.2) profiles, with coincidence defined as being within plus or minus 2 degrees  
7 of latitude, 8 degrees of longitude, and on the same day. The 3 methods used to place the  
8 finer vertical resolution SAGE II profiles on the MLS retrieval grid are (a) simple  
9 interpolation versus log (pressure), (b) a least-squares fit of SAGE II ozone profiles onto  
10 the MLS retrieval grid, and (c) an additional smoothing of the least-squares-fitted profiles  
11 using the MLS vertical averaging kernels (section 2.4), following the methodology of  
12 *Rodgers* [1976], and expanded upon by *Rodgers and Connor* [2003]. Differences of only  
13 a few percent among the three methods exist for pressures less than 100 hPa, with  
14 somewhat bigger differences observed at larger pressures. Similar conclusions, but using  
15 MLS ozone versus ozonesonde profiles, are provided by *Jiang et al.* [2007]. In the  
16 stratosphere, and down to a pressure level of 147 hPa, the average differences between  
17 MLS and SAGE II data are within a few to 7%.

18 The results of comparisons between SAGE II average profiles (using the least-squares  
19 fits of the fine resolution profiles) and MLS averaged coincident profiles are given in  
20 Figure 11, with curves to compare the standard deviations of the differences and the  
21 combined estimated precisions, the latter being obtained from the root sum square (rss) of  
22 the (random) uncertainties provided in the MLS and SAGE II data files. The standard  
23 deviations of the differences can be as low as 5% in the stratosphere, with significant

1 increases at the lowest altitudes reflecting increased atmospheric variability, as the  
2 expected combined precisions are significantly lower than the standard deviations in this  
3 region. We can find better agreement between the precisions and the standard deviations  
4 if we assume a larger precision for the SAGE II profiles. *Borchi et al.* [2005] estimate  
5 that the SAGE II precision is about 2 to 3%, but the uncertainty values from the SAGE II  
6 files are often significantly smaller than this, and therefore, the combined precisions  
7 shown in Figure 11 are probably an underestimate. We see this pattern in many of the  
8 subsequent comparisons, with precision estimates on the low end of the scatter values  
9 given by the standard deviations of the differences.

10 Results of the coincident profile comparisons, binned in ten degree latitude bins, are  
11 plotted as a function of latitude in Figure 12. The latitudinal behavior is tracked in a very  
12 similar fashion by both sets of data. This is also illustrated by the contour plot of Figure  
13 13, which only uses data from January through March, 2005, when a larger set of nearly  
14 contiguous days (32 total) was reprocessed to v2.2 data. Figure 12 shows that MLS  
15 tropical ozone values (for latitudes 20°S to 20°N) are significantly larger than those from  
16 SAGE II at 100 to 215 hPa. While part of this accentuated percent difference arises from  
17 low ozone values in these regions, a positive bias is present. SAGE II ozone values have  
18 been shown to be significantly (up to 50%) low versus ozonesonde data (for  
19 Hohenpeissenberg at 47°N) near and below the tropopause [*P.-H. Wang et al.*, 2006], so  
20 the fact that MLS values at 215 hPa are larger than SAGE II by 10-20% at mid-to high  
21 latitudes (Figure 12) does not demonstrate that an absolute bias exists in the MLS data.  
22 In a companion paper, *Jiang et al.* [2007] show that v2.2 ozone has a high average bias  
23 versus ozonesonde data at 215 hPa, by 20 to 40%, but a much smaller bias (of order 5%)

1 is observed versus lidar measurements (down to 215 hPa) from the Table Mountain  
2 Facility, in California. Additional studies of the low altitude MLS data using  
3 comparisons versus aircraft ozone data are discussed later in this paper and by *Livesey et al.*  
4 *[2007]*.

### 5 ***MLS and HALOE Profiles***

6 In the following comparisons with other satellite instrument ozone data, we use the  
7 least-squares fit method for smoothing the correlative data sets. Results of such  
8 comparisons are given in Figures 14, showing global percent differences between MLS  
9 and the solar occultation infrared measurements by HALOE [*Russell, et al., 1993*]; we  
10 use publically available HALOE version 19 data, and the vertical resolution for O<sub>3</sub> is  
11 about 2 km. The two panels in Figure 14 separate the results of the comparisons using  
12 day and night MLS profiles (top panel) and daytime only MLS profiles (bottom panel), as  
13 mesospheric comparisons require additional care because of diurnal changes in that  
14 region. Indeed, *Boyd et al. [2007]* point out that daytime observations should give better  
15 agreement with HALOE twilight observations in the mesospheric region, which has  
16 elevated nighttime ozone; Figure 14 illustrates that this is indeed the case. Ultimately,  
17 however, ground-based microwave observations should provide the best means of  
18 validating the day and night MLS ozone abundances, and related variations in the upper  
19 stratosphere and mesosphere. *Hocke et al. [2006]* have demonstrated good agreement in  
20 MLS v1.5 comparisons versus ground-based microwave data from Switzerland.  
21 Excellent agreement (most often within 5%) is also found between MLS v2.2 data and  
22 ozone from the ground-based microwave measurements at Mauna Loa, Hawaii and  
23 Lauder, New Zealand, as discussed by *Boyd et al. [2007]*. We note that HALOE

1 retrievals take into account variations along the line of sight in (twilight) mesospheric  
2 ozone, whereas the other satellite occultation instrument retrievals do not (to our  
3 knowledge); however, the impact of twilight gradients on HALOE mesospheric ozone  
4 could still be as large as 20% (for sunrise occultations in particular), if improved  
5 treatment of these effects were to be included in the HALOE retrievals [*Natarajan et al.*,  
6 2005]. The stratospheric MLS/HALOE ozone comparisons shown in Figure 14 are  
7 slightly poorer than the MLS/SAGE II comparisons, but still very good (within 5%  
8 between 68 and 2 hPa), with the HALOE values slightly lower than those from MLS.  
9 This level of agreement is not surprising, as the SAGE II and HALOE ozone  
10 measurements often agree to within about 5%, with HALOE ozone values typically also  
11 slightly lower than the SAGE II values [e.g., *Nazaryan et al.*, 2005]; however, results of  
12 the HALOE/SAGE II comparisons in the latter reference are not given below 20 km. At  
13 the largest pressures shown here (100 and 147 hPa), the MLS values are larger than the  
14 HALOE values by 15% on average. Figure 15 gives latitudinal comparisons for the  
15 matched MLS/HALOE profile pairs and indicates good comparisons at mid- to high  
16 latitudes, with larger differences arising at low latitudes, where there are also few  
17 coincident profiles. *Bhatt et al.* [1999] have noted that comparisons of ozonesonde  
18 profiles versus HALOE data give good results (within about 10%) down to 100 hPa at  
19 low latitudes, and down to 200 hPa at extratropical latitudes. However, HALOE tends to  
20 show low values versus ozonesondes at the highest pressures, and interference from  
21 aerosols or cirrus significantly reduces the number of available profiles for pressures  
22 larger than 100 hPa. In terms of precisions, we observe in Figure 14 that the standard  
23 deviation of the differences in the stratosphere can get to within two percent of the

1 estimated combined precision, but is on the high side of the precision estimate. This is  
2 probably for reasons similar to those mentioned for SAGE II comparisons (imperfect  
3 coincidences and real atmospheric variability, and possibly, some underestimate of the  
4 HALOE precisions).

### 5 ***MLS and ACE-FTS Profiles***

6 Figures 16 and 17 show analyses similar to those in Figures 11 and 12 for SAGE II,  
7 but for MLS ozone versus the Atmospheric Chemistry Experiment Fourier Transform  
8 Spectrometer (ACE-FTS) ozone results during 2004 through 2006; this longer time  
9 period (for ACE data) allows for comparisons with close to 130 days of MLS v2.2 data  
10 (at the time of writing), about double the number of MLS v2.2 days that were available  
11 for the SAGE II comparisons. ACE-FTS on the Canadian Space Agency's SCISAT  
12 mission [Bernath *et al.*, 2005] provides retrievals [Boone *et al.*, 2005] since February  
13 2004 for ozone and many other species from solar occultation observations at high  
14 resolution ( $0.02\text{ cm}^{-1}$ ) in the infrared (2 to 13  $\mu\text{m}$ ); the ACE-FTS vertical resolution for  
15 ozone is close to 4 km, and the retrievals are provided on a 1 km vertical grid. In the  
16 upper stratosphere, we observe somewhat larger average differences (in Figure 16), in  
17 comparison to MLS versus SAGE II or HALOE, between MLS and the ACE-FTS  
18 version 2.2 ozone "update", which includes modifications to retrieve ozone using  
19 "microwindows" only in the 10  $\mu\text{m}$  spectral region. The MLS/ACE differences are small  
20 (within  $\sim 5\%$ ) in the lower stratosphere, but increase with altitude and are largest in the  
21 upper stratosphere. The MLS results in that region agree generally better with other  
22 satellite datasets (see also further below), as well as with ground-based lidar (Jiang *et al.*  
23 [2007]) and microwave [Hocke *et al.*, 2006; Boyd *et al.*, 2007] measurements in that

1 region. The apparent high bias in ACE-FTS upper stratospheric ozone was noticed in  
2 v1.0 ACE-FTS data [Walker *et al.*, 2005], persists in the v2.2 ACE data version, as well  
3 as in a sampling of the latest (v3.0) ACE retrievals. Some (maybe most) of this could be  
4 caused by the difficulty associated with retrieving at twilight (during solar occultation)  
5 when the line-of-sight gradients in ozone are strong enough to perturb retrievals that  
6 assume a homogeneous atmosphere. The standard deviation of the differences in Figure  
7 16 are, as in the previous comparisons versus SAGE II and HALOE, an upper limit for  
8 the estimated combined precision. The latitudinal variations of these coincident (and  
9 averaged) profiles agree quite well, as demonstrated in Figure 17; this is also  
10 demonstrated, as a function of equivalent latitude, by Manney *et al.* [2007].

### 11 ***MLS and POAM III Profiles***

12 We also compare MLS ozone versus the high latitude measurements from POAM III,  
13 which uses solar occultation observations at UV/visible wavelengths to provide ozone  
14 profiles with a vertical resolution of about 1 km; version 4 POAM III data are used here.  
15 Previous validation studies have documented POAM III stratospheric ozone data as being  
16 of high quality; see Randall *et al.* [2003] and Lumpe *et al.* [2003]. The MLS/POAM III  
17 comparisons in Figure 18 show better than 5% agreement on average, from 100 to 1 hPa.  
18 Comparisons in the mesosphere are slightly poorer, in terms of average percent  
19 differences, but again, this region is complicated by diurnal changes in ozone and the  
20 potential for larger solar occultation retrieval errors caused by rapidly changing ozone  
21 along the line of sight.

### 22 ***MLS and MIPAS Profiles***

1           The Michelson Interferometer for Passive Atmospheric Sounding (MIPAS)  
2 [*Fischer and Oelhaf*, 1996] was launched on the European Space Agency (ESA)  
3 Environmental Satellite (Envisat) in March 2002 into a 98.5 degree inclination orbit.  
4 MIPAS is a Fourier Transform Spectrometer detecting limb emission in the infrared  
5 spectral region 685-2410  $\text{cm}^{-1}$  (4.1-14.6  $\mu\text{m}$ ) with a spectral resolution of 0.025  $\text{cm}^{-1}$ .  
6 MIPAS operations were suspended in March 2004 due to an interferometer mechanism  
7 anomaly and restarted in January 2005 with a degraded spectral resolution of 0.0625 $\text{cm}^{-1}$   
8 and modified duty-cycle and scan sequence to extend instrument lifetime [*Piccolo and*  
9 *Dudhia*, 2007]. MIPAS observes temperature, aerosols and a large number of minor  
10 constituents, including ozone. The horizontal along-track sampling interval of the MIPAS  
11 measurements taken in the nominal reduced-resolution mode is  $\sim 410$  km, latitude  
12 coverage is 90°S to 90°N, and the vertical sampling is 1.5 to 4 km with a vertical range of  
13 6 to 70 km. In addition to the ESA operational data products [*Raspollini et al.*, 2006],  
14 several institutions funded by the ENVISAT Calibration/Validation Program have  
15 developed off-line data processing capabilities for MIPAS. Here we show comparisons  
16 with off-line MIPAS ozone retrievals from algorithms developed at the University of  
17 Oxford [personal communication, A. Dudhia and C. Waymark, 2006]. The MIPAS  
18 profiles were supplied with a cloud flag, that has been used for data screening.

19           In Figure 19, a single day (28 January, 2005) of retrievals from the MIPAS  
20 measurements is compared to the ozone data from the same day for MLS. These results  
21 are generally in very good agreement, although in the mid-stratosphere the MIPAS values  
22 are larger than MLS by about 10%. This difference does not show the same  
23 characteristics as the upper stratospheric bias between MLS and ACE-FTS shown earlier,

1 and we do not see such a bias versus SAGE II (Figure 11), HALOE (Figure 14), ground-  
2 based lidars [*Jiang et al.*, 2007], or ground-based microwave data [e.g., *Boyd et al.*,  
3 2007]. These limited comparisons show average agreement within 10%, as well as good  
4 latitudinal correspondence (although not shown here) in both the stratosphere and lower  
5 mesosphere, with increases into the polar night at high altitude (up to 0.05 hPa). This  
6 helps confirm that MLS mesospheric retrievals are worth using for scientific studies,  
7 given this kind of agreement between emission measurements from different wavelength  
8 regions. However, more detailed comments about MIPAS and MLS differences or biases  
9 should await further work, as we are not aware of other related validation for this limited  
10 dataset. However, the recent study by *Boyd et al.* [2007] provides comparisons of  
11 ground-based microwave ozone data versus MIPAS operational ozone retrievals, as well  
12 as versus MLS ozone, for altitudes up to about 70 km.

### 13 ***MLS Column Ozone Abundances***

14 *Yang et al.* [2007] have shown that the MLS v1.5 column ozone abundances calculated  
15 down to the tropopause give excellent agreement with SAGE II columns and are often  
16 slightly (a few DU) larger than the SAGE II column values, for MLS columns down to  
17 215 hPa in particular; that analysis also shows that SAGE III and HALOE ozone columns  
18 depart slightly more from MLS, but straddle both the SAGE II and the MLS v1.5 values.  
19 The slight reduction in the MLS v2.2 column values brings SAGE II and MLS columns  
20 into even better agreement. *Petropavlovskikh et al.* [2007] have performed comparisons  
21 of MLS column abundances with aircraft-based column ozone data from the CAFS  
22 instrument on several Aura Validation Experiment (AVE) campaigns. They find that the

1 columns agree within a few percent and that both measurements track atmospheric  
2 changes along the aircraft trajectories (during Aura overpasses) quite well.

3 Figure 20 shows a comparison between MLS column abundances and the SAGE II  
4 column abundances, for coincident profiles using available (reprocessed) v2.2 MLS data  
5 and SAGE II profiles from August 2004 to August 2005. *Jiang et al.* [2007] have  
6 compared MLS partial column abundances to ozonesonde partial columns; they find that  
7 the results are somewhat poorer than the results shown here for SAGE II versus MLS.  
8 This may be because the columns calculated for the SAGE II comparisons extend higher  
9 in altitude than for the typical sonde comparisons, and some compensation may occur  
10 when including MLS ozone values (up high) that may be biased slightly lower than  
11 SAGE II ozone in that region.

### 12 **3.2 Comparisons with Balloon Data**

13 Comparisons between MLS data and measurements from balloons launched from  
14 Ft. Sumner, New Mexico, in September, 2004, have been discussed by *Froidevaux et al.*  
15 [2006a]. The small changes between MLS v1.5 and v2.2 ozone do not alter the  
16 conclusion from that work regarding good overall agreement; for example, there is  
17 typically better than ~5% agreement between MLS v2.2 ozone from 100 to 10 hPa and  
18 the September, 2004, in situ UV photometer balloon data, whose accuracy is estimated to  
19 be under 5%. Another large balloon campaign was carried out from Ft. Sumner in  
20 September, 2005; see *Froidevaux et al.* [2006a] for a brief description of the various  
21 balloon-borne instruments, excluding the JPL Submillimeterwave Limb Sounder-2 (SLS-  
22 2), which did not fly in 2004. The latter instrument provides profiles of various trace  
23 gases, including ozone, from scans of the Earth's limb thermal emission near 600 GHz.

1 This new instrument includes cooled components and provides much greater sensitivity  
2 than an earlier SLS instrument. A vertical resolution of 2 to 3 km is achieved by SLS-2  
3 and the other remote sensing balloon instruments discussed here, the JPL MkIV Fourier  
4 Transform Infrared (FTIR) spectrometer, which performs solar occultation observations  
5 in the 650 to 5650  $\text{cm}^{-1}$  region at 0.01  $\text{cm}^{-1}$  spectral resolution [Toon, 1991], and the  
6 Smithsonian Astrophysical Observatory (SAO) far-infrared spectrometer FIRS-2,  
7 measuring thermal emission at 6 to 120  $\mu\text{m}$  with a spectral resolution of 0.004  $\text{cm}^{-1}$   
8 [Johnson *et al.*, 1995]. As in 2004, this flight lasted over 18 hours at float, and sunset  
9 occultation data were obtained by the MkIV instrument. Figure 21 displays ozone  
10 measurements from this flight, in comparison to the closest daytime and nighttime ozone  
11 profiles from MLS. Again, we find very good agreement, with MLS profiles falling in  
12 the midst of the balloon measurements, which differ among themselves by more than 5%  
13 in places. The change in slope near 15 hPa in the in situ profile is captured by the MLS  
14 retrievals, although the MLS values are 5 to 9% larger near the ozone peak, as are most  
15 of the other balloon profiles, possibly because of atmospheric inhomogeneities. On  
16 average, the MLS results between 215 and 3 hPa are 4% larger than the in situ  
17 photometer data, with a standard deviation of 7%. The MkIV profile peak occurs below  
18 the peaks in the profiles from MLS, FIRS-2 and SLS, possibly because the MkIV solar  
19 occultation measurements sample a different atmospheric region than the balloon  
20 emission instruments. These results are useful in confirming the validity of MLS ozone.  
21 However, not enough statistics have been provided by large balloons since the Aura  
22 launch to enable robust conclusions regarding biases that might exceed the previously  
23 discussed stratospheric MLS ozone accuracy estimates of 5 to 7%, which should be

1 combined with the accuracy estimates (typically also 5 to 10%) from the balloon  
2 instruments, whose measurements often vary by as much as the (small) differences  
3 observed versus MLS.

### 4 **3.3 Comparisons with Aircraft Data**

5 One of the high priority requests for validation data from campaigns in support of the  
6 Aura measurements of ozone profiles, as part of the pre-launch planning for Aura  
7 validation [*Froidevaux and Douglass, 2001*], was aircraft lidar measurements along the  
8 sub-orbital MLS track, in order to compare “curtain plots” retrieved from the lidar and  
9 satellite instruments. A series of such comparisons was enabled in a powerful way  
10 during the campaign of January/February, 2005, named Polar Aura Validation  
11 Experiment (or PAVE), during which the NASA DC-8 conducted several flights into the  
12 Arctic polar vortex. Both the airborne Differential Absorption Lidar (DIAL) and the  
13 Airborne Raman Ozone, Temperature, and Aerosol Lidar (AROTAL) instruments were  
14 onboard the DC-8 during the flights, portions of which were often planned to coincide  
15 with the MLS sub-orbital track. Airborne lidar measurements from DIAL and AROTAL  
16 have a long history [e.g., *Browell et al.*, 1990, 1998, 2003, *McGee et al.*, 1995, *Lait et al.*,  
17 2004]. *Schoeberl et al.* [2006b] illustrate some of the atmospheric features, including  
18 polar vortex filamentation, observed by both the aircraft and Aura MLS during the PAVE  
19 campaign. AROTAL uses Rayleigh scattered signals from a pair of lasers transmitting at  
20 308 and 355 nm to measure ozone, temperature, and aerosols. Lidar data are acquired in  
21 15 m bins, read out every 20 s, and integrated for several minutes, to provide a running  
22 mean ozone profile every 20s. The vertical resolution varies between 0.75 and 3 km.  
23 The DIAL instrument utilizes two lasers (using 301 and 310 nm wavelengths) and

1 provides ozone data at (typically) 0.5 to 0.7 km vertical resolution above and below the  
2 aircraft, with a roughly 0.75 km gap just above and below the aircraft altitude; this gap  
3 has been filled in by interpolation, using in situ data from the Fast-Response Ozone  
4 (FASTOZ) measurements aboard the aircraft [see also *Browell et al.*, 2003]. The  
5 archived DIAL data are provided roughly for every minute of flight time (or about 14 km  
6 horizontal distance), based on 5-minute running averages. Lidar ozone mixing ratios are  
7 calculated from the ozone number densities (the original lidar retrievals) and the Goddard  
8 Space Flight Center (GSFC) Assimilation gridded atmospheric density profiles  
9 interpolated along the aircraft flight track (kindly provided by GSFC codes 610.1 and  
10 613.3). The aircraft flights were timed to have the Aura overpass occur within the  
11 flights' temporal extent, which typically lasted a number of hours as opposed to the  
12 timescale for satellite overpass (at 7 km/s), lasting only a minute or two over the region  
13 covered by the aircraft.

14 Figure 22 shows a map with the aircraft tracks (solid black) north of Portsmouth,  
15 New Hampshire (the DC-8 base for this campaign), and with superimposed MLS profile  
16 locations (colored dots) for the flights of 27 January, 31 January, and 5 February, 2005.  
17 We have used these three days as providing the best coincident measurements from the  
18 lidars and MLS during the PAVE campaign; the two legs of close coincidence with the  
19 two MLS daytime tracks on February 5 are spaced by about one hour and a half, and are  
20 both used in our comparisons. Figures 23, 24, and 25 show results from the lidar and  
21 MLS ozone comparisons. The lidar data have been smoothed using a two-dimensional  
22 least-squares routine to compare on the same grid (horizontal and vertical) as the MLS  
23 profiles. The latter two figures give percent differences for 31 January and 27 January.

1 Figure 26 shows a summary of the average profiles for all 4 flight legs shown in Figure  
2 22; the MLS values corresponding to the averages of the (smoothed) DIAL and  
3 AROTAL profiles are shown as open circles; occasional bad lidar data can produce slight  
4 differences in the averages that are appropriate for the two lidar data sets. AROTAL lidar  
5 measurements can be used at somewhat higher altitudes than the DIAL data, and the  
6 DIAL data, coupled with FASTOZ measurements are used for the higher pressures (at  
7 and below the aircraft). Percentage differences between MLS and DIAL or AROTAL  
8 profiles, as well as standard deviations of the differences are shown in the right panel of  
9 Figure 26; the error bars on these points indicate twice the precision (standard error) in  
10 the mean differences, based on the MLS precision values and a value of 5% precision to  
11 account for the lidar uncertainty, including the translation of ozone abundances to mixing  
12 ratios versus pressure via the meteorological “curtain files” provided by GSFC as part of  
13 this campaign’s archived data. There are enough statistics in these comparisons to make  
14 differences stand out above the random uncertainties (not counting systematic errors).  
15 The MLS averages between 20 and 150 hPa are very close to (within 6% of) both  
16 AROTAL and DIAL measurements. These differences are within the combined  
17 accuracies of the MLS and lidar data. The MLS average high bias at 215 hPa is not as  
18 clearly evident in comparisons of MLS ozone with the downward-looking DIAL during  
19 the Spring of 2006 Intercontinental Chemical Transport Experiment-B (INTEX-B)  
20 campaign [Livesey *et al.*, 2007].

21 Figure 27 shows “curtain plots” and percent differences versus AROTAL data  
22 gathered during the INTEX-B DC-8 nighttime transit flight from Hawaii to Anchorage,  
23 Alaska, on 1 May, 2006. Portions of the lidar data file with no data (or bad data) for this

1 flight may be causing a few undesirable effects during the smoothing process for these  
2 comparisons, and the flight track was more removed (by up to a few degrees for the  
3 latitudes shown here) from the MLS track than during the PAVE flights. However, the  
4 average MLS/lidar differences from 100 to 10 hPa are within 5 to 10% for this flight,  
5 with standard deviations of 5% (near 20 hPa) to 18% (at 100 hPa). Both instruments  
6 observe very similar gradients from the tropical latitudes to midlatitudes, notably in the  
7 lower stratosphere. Another nighttime flight (also targeted more at the HIRDLS track)  
8 occurred on 22 March, 2006, during transit from Houston to NASA Ames. The results of  
9 the MLS and AROTAL comparisons for this flight are shown in Figure 28. Again, the  
10 differences are fairly small and excellent agreement is obtained: average differences are  
11 within 6% for 7 to 46 hPa, and 10% at 68 hPa, with standard deviations from 4% to 12%  
12 at all heights. On average, these two nighttime flights give differences between MLS and  
13 AROTAL that are within 2% from 10 hPa to 46 hPa, and 6% and 10% (MLS slightly  
14 lower than AROTAL) for 68 hPa and 100 hPa, respectively. A daytime DC-8 flight  
15 coincidence with the MLS track (from about 34°N to 44°N) on April 25, 2006 gives  
16 slightly larger (10-15%) differences between MLS and AROTAL over a narrower  
17 available vertical range (details not shown here), probably because of difficulties in  
18 obtaining optimum lidar background calibration under large solar flux conditions (high  
19 sun); the observed horizontal gradients on that day are still quite similar for the two  
20 datasets.

21 Overall, we find that the combination of lidar and MLS ozone data during such  
22 aircraft campaigns successfully demonstrates that the satellite and aircraft measurements  
23 offer a similar view of the atmosphere, despite their vastly different raw measurement

1 characteristics. The validity of MLS ozone data, within the precision and accuracy  
2 estimates we provide in this work, seem to be borne out as a result of the majority of  
3 these comparisons. Of course, the finest resolution views are not possible with MLS, and  
4 the broad daily coverage is not possible from the aircraft, so the satellite/aircraft  
5 combination provides a suite of complementary measurements.

## 6 7 **4 Summary and Conclusions**

8  
9 We remind MLS data users to apply the data screening criteria discussed in this  
10 paper (section 2.3) for the version 2.2 ozone data, as there have been some changes from  
11 the screening for version 1.5.

12 Table 2 gives a summary of the estimated resolution, precision, and accuracy of  
13 MLS v2.2 ozone. Some of the results given in this Table overlap with the results  
14 regarding MLS ozone at the highest pressures (upper troposphere and lower portion of  
15 the stratosphere), which are the focus of the analyses by *Livesey et al.* [2007], and include  
16 a number of comparisons versus the INTEX-B aircraft campaign results (from DIAL and  
17 in situ ozone data). The accuracy for 215 hPa has been increased from its theoretical  
18 estimate of 20 ppbv + 10% to 20 ppbv + 20%, based mainly on the results of MLS  
19 comparisons versus ozonesondes [*Jiang et al.*, 2007], and as discussed further below.

20 The MLS standard ozone product from the version 2.2 retrievals is in very good  
21 agreement with other well established data sets. Over much of the stratosphere (from 1 to  
22 100 hPa), the estimated accuracy of MLS ozone is about 8% or better, based on  
23 sensitivity estimates using different options for input parameters to the MLS retrievals,  
24 and consistent with comparisons to well established satellite ozone data sets and to

1 ozonesondes [see *Jiang et al.*, 2007]. For example, results of MLS v2.2 ozone  
2 comparisons versus SAGE II ozone show agreement within a few to 7% for the  
3 stratosphere, and as low down as 147 hPa. Some high MLS biases (~20% globally) are  
4 apparent at 215 hPa (the bottom recommended level for MLS), in comparisons versus  
5 ozonesondes [*Jiang et al.*, 2007]. A systematic MLS bias at 215 hPa of about 10-20% is  
6 also indicated by the MLS comparisons with SAGE II and PAVE lidar data, although this  
7 is not discerned from MLS and aircraft in situ and DIAL lidar ozone comparisons during  
8 the INTEX-B campaign [*Livesey et al.*, 2007].

9         Other recent analyses of MLS and solar occultation data (including SAGE III) by  
10 *Manney et al.* [2007] support the statements made here regarding the quality of the MLS  
11 standard ozone product. Furthermore, excellent agreement (mostly within ~5%) is  
12 obtained in comparisons between MLS and ground-based microwave data into the  
13 mesosphere [*Hocke et al.*, 2006; *Boyd et al.*, 2007]. The upper stratospheric and lower  
14 mesospheric differences in average (coincident profile) abundances observed by MLS  
15 and several of the solar occultation instruments (SAGE II, POAM III, and ACE-FTS)  
16 indicate that there are more difficulties associated in comparisons between occultation  
17 retrievals, when significant line-of-sight gradients exist along the absorption ray paths,  
18 with measurements from thermal emission, such as from MLS, MIPAS, or ground-based  
19 microwave. Further careful mesospheric ozone comparisons between MLS and MIPAS,  
20 or using mesospheric measurements from the Sounding of the Atmosphere with  
21 Broadband Emission Radiometry (SABER) or the Global Ozone Monitoring by  
22 Occultation of Stars (GOMOS) experiments could prove useful in expanding  
23 mesospheric validation efforts, beyond the scope of this paper.

1           The MLS stratospheric column ozone abundances have been shown to be in  
2 excellent agreement with SAGE II column ozone data, which confirms the results of  
3 *Ziemke et al.* [2006] and *Yang et al.* [2007], who used mostly v1.5 MLS data. MLS  
4 column abundances have also been shown to be in good agreement (within a few percent)  
5 with aircraft measurements [*Petropavlovskikh et al.*, 2007], and ozonesonde partial  
6 columns [*Jiang et al.*, 2007], although a slight (less than 2 or 3%) high MLS bias is  
7 evident in some of the comparisons from the latter reference. *Schoeberl et al.* [2007b]  
8 also discuss a possible high MLS bias in their analyses of MLS v1.5 column data.  
9 However, the stratospheric MLS columns have been reduced in v2.2 (by 0.5 to 2%), in  
10 comparison to v1.5 MLS column data, mitigating but maybe not always eliminating such  
11 column biases.

12           The latitudinal distributions obtained by satellite (coincident) profiles and the  
13 aircraft-based lidar “curtains” along the sub-orbital MLS track show very good  
14 agreement with MLS distributions, with a few small offsets in places. Results of detailed  
15 temporal comparisons await more studies with additional version 2.2 MLS data, but 5%  
16 agreement with other satellite data sets must imply that there is overall good tracking of  
17 seasonal changes, for example, although this is not shown here. Good agreement in  
18 ozone temporal variations from 2004 to 2006 between MLS (v1.5) data and sample data  
19 from ozonesonde and lidar (at northern midlatitudes) is illustrated by *Jiang et al.* [2007].  
20 We have also shown here (see Figure 9) that the v2.2 MLS data track the v1.5 MLS data  
21 very well as a function of time, based on available data at the time of writing.  
22 Furthermore, accurate information about stratospheric variations on timescales of the

1 quasi-biennial oscillation (QBO) are now emerging from the Aura MLS data set  
2 [*Schoeberl et al.*, 2007a].

3         The MLS ozone measurements have also been shown to significantly improve  
4 data assimilation results in comparison to assimilation without MLS [*Stajner et al.*, 2007;  
5 *Jackson*, 2007]. We certainly expect that much more knowledge will be forthcoming in  
6 years to come, based on MLS and Aura ozone data in general, regarding stratospheric and  
7 tropospheric ozone variations, with connections to the issue of air quality from regional  
8 to global scales, as well as to climate change.

9

10

1

2 **Table 2.** Summary of MLS v2.2 ozone characteristics at selected pressure levels

| Pressure<br>hPa | Resolution<br>Vert.x Horiz. <sup>a</sup><br>km | Precision <sup>b</sup> |       | Accuracy <sup>c</sup> |       | Comments                                                                      |
|-----------------|------------------------------------------------|------------------------|-------|-----------------------|-------|-------------------------------------------------------------------------------|
|                 |                                                | ppmv                   | %     | ppmv                  | %     |                                                                               |
| ≤ 0.01          | -----                                          | -----                  | ----- | -----                 | ----- | Not recommended for scientific use                                            |
| 0.02            | 6 x 200                                        | 1.0                    | 200   | 0.1                   | 35    |                                                                               |
| 0.05            | 6 x 200                                        | 0.6                    | 100   | 0.2                   | 30    |                                                                               |
| 0.1             | 4 x 300                                        | 0.4                    | 40    | 0.2                   | 20    |                                                                               |
| 0.2             | 3 x 300                                        | 0.4                    | 30    | 0.1                   | 7     |                                                                               |
| 0.5             | 3 x 300                                        | 0.3                    | 15    | 0.1                   | 5     |                                                                               |
| 1               | 3 x 250                                        | 0.3                    | 10    | 0.2                   | 7     |                                                                               |
| 2               | 3 x 250                                        | 0.2                    | 5     | 0.2                   | 5     |                                                                               |
| 5               | 3 x 200                                        | 0.2                    | 3     | 0.3                   | 5     |                                                                               |
| 10              | 3 x 200                                        | 0.2                    | 3     | 0.3                   | 5     |                                                                               |
| 22              | 3 x 200                                        | 0.1                    | 2     | 0.2                   | 5     |                                                                               |
| 46              | 3 x 200                                        | 0.1                    | 4     | 0.2                   | 8     |                                                                               |
| 68              | 3 x 200                                        | 0.05                   | 3-10  | 0.05                  | 3-10  |                                                                               |
| 100             | 3 x 200                                        | 0.04                   | 2-30  | 0.05 +                | 5%    |                                                                               |
| 150             | 3 x 200                                        | 0.04                   | 5-100 | 0.02 +                | 5%    |                                                                               |
| 215             | 3 x 200                                        | 0.04                   | 5-100 | 0.02 +                | 20%   |                                                                               |
| > 300           | -----                                          | -----                  | ----- | -----                 | ----- | Not recommended for scientific use<br>(not retrieved for pressures > 316 hPa) |

3 <sup>a</sup> Horizontal resolution is in the along-track direction, and the (along-track) separation between  
 4 adjacent retrieved profiles is 1.5° great circle angle (~165 km); cross-track resolution is ~6 km.

5 <sup>b</sup> Precision is 1σ estimate for individual profiles.

6 <sup>c</sup> Systematic uncertainty, 2σ estimate of probable magnitude (see text).

1

## 2 **Acknowledgments**

3 This work at the Jet Propulsion Laboratory, California Institute of Technology, was  
4 performed under contract with the National Aeronautics and Space Administration. We  
5 are very grateful to the MLS instrument and data/computer operations and development  
6 team (at JPL and from Raytheon, Pasadena) for their support through all the phases of the  
7 MLS project, in particular D. Flower, G. Lau, J. Holden, R. Lay, M. Loo, G. Melgar, D.  
8 Miller, B. Mills, M. Echeverri, E. Greene, A. Hanzel, A. Mousessian, S. Neely, C. Vuu,  
9 and P. Zimdars. We greatly appreciate the efforts of B. Bojkov and the Aura Validation  
10 Data Center (AVDC) team, whose work facilitated the MLS validation activities. We  
11 thank A. Dudhia and C. Waymark at Oxford University for their role in providing  
12 MIPAS ozone retrievals discussed in this work, and I. Boyd and A. Parrish for comments  
13 on day and night mesospheric ozone comparisons. We also acknowledge the work of the  
14 satellite instrument and science teams from SAGE II, HALOE, and POAM III, who  
15 provided readily available high quality data that helped us provide timely validation  
16 analyses for the MLS retrievals. Thanks to the Aura Project for their support throughout  
17 the years (before and after the Aura launch), in particular M. Schoeberl, A. Douglass  
18 (also as co-chair of the Aura validation working group), E. Hilsenrath, and J. Joiner. We  
19 also acknowledge the support from NASA Headquarters, P. DeCola for MLS and Aura,  
20 and M. Kurylo, J. Gleason, B. Doddridge, and H. Maring, especially in relation to the  
21 Aura validation activities and campaign planning efforts. The aircraft campaigns  
22 themselves involved tireless hours of planning from various coordinators, including  
23 E. Jensen, M. Schoeberl, H. Singh, D. Jacob, and others, as well as K. Thompson and  
24 others involved with campaign flight management and support. We express our thanks to

1 the DIAL, AROTAL, and FASTOZ instrument and data analysis teams for their efforts in  
2 association with the PAVE field experiment, and to the Columbia Scientific Balloon  
3 Facility for launching the balloon experiments whose data are used in this work. Funding  
4 for ACE was provided by the Canadian Space Agency and the Natural Sciences and  
5 Engineering Research Council (NSERC) of Canada.

1

2 **References**

- 3 Barret, B., et al. (2006), Intercomparisons of trace gases profiles from the Odin/SMR and  
4 Aura/MLS limb sounders, *J. Geophys. Res.*, 111, D21302,  
5 doi:10.1029/2006JD007305.
- 6 Bernath, P.F., et al. (2005), Atmospheric Chemistry Experiment (ACE): Mission  
7 overview, *Geophys. Res. Lett.*, 32, L15S01, doi:10.1029/2005GL022386.
- 8 Bhatt, P. P., E. E. Remsberg, L. L. Gordley, J. M. McInerney, V. G. Brackett, and J. M.  
9 Russell III (1999), An evaluation of the quality of Halogen Occultation Experiment  
10 ozone profiles in the lower stratosphere, *J. Geophys. Res.*, 104, 9261-9275.
- 11 Boone, C.D., et al. (2005), Retrievals for the Atmospheric Chemistry Experiment  
12 Fourier-Transform Spectrometer, *Appl. Opt.*, 44, 7218-7231.
- 13 Borchi, F., J.-P. Pommereau, A. Garnier, and M. Pinharanda (2005), Evaluation of  
14 SHADOZ sondes, HALOE and SAGE II ozone profiles at the tropics from SAOZ  
15 UV-Vis remote measurements onboard long duration balloons, *Atmos. Chem. Phys.*,  
16 5, 1381-1397.
- 17 Boyd, I.S., et al. (2007), Ground Based Microwave Ozone Radiometer Measurements  
18 Compared with Aura-MLS v2.2 and Other Instruments at Two NDACC Sites, *J.*  
19 *Geophys. Res.*, submitted to this special issue.
- 20 Browell, E. V., et al. (1990), Airborne lidar observations in the wintertime Arctic  
21 stratosphere: Ozone, *Geophys. Res. Lett.*, 17, 325-328.
- 22 Browell, E. V., S. Ismail, and W. B. Grant (1998), Differential Absorption Lidar (DIAL)  
23 measurements from air and space, *Appl. Phys. B*, 67, 399-410.
- 24 Browell, E. V., et al. (2003), Large-scale ozone and aerosol distributions, air mass  
25 characteristics, and ozone fluxes over the western Pacific Ocean in late winter/early  
26 spring, *J. Geophys. Res.*, 108, doi:10.1029/2002JD003290.
- 27 Fisher, H., and H. Oelhaf (1996), Remote sensing of vertical profiles of atmospheric trace  
28 constituents with MIPAS limb-emission spectrometers, *Appl. Opt.*, 35, 2787-2796.
- 29 Froidevaux, L., et al. (1996), Validation of UARS Microwave Limb Sounder ozone  
30 measurements, *J. Geophys. Res.*, 101, 10,017-10,060.
- 31 Froidevaux, L., and A. Douglass (2001), eds., Earth Observing System (EOS) Aura  
32 Science Data Validation Plan, Report, Version 1.0, NASA Goddard Space Flight  
33 Center, Greenbelt, MD.
- 34 Froidevaux, L., et al. (2006a), Early validation analyses of atmospheric profiles from  
35 EOS MLS on the Aura satellite, *IEEE Trans. Geosci. Remote Sensing*, 44, No. 5,  
36 1106-1121.
- 37 Froidevaux, et al. (2006b), Temporal decrease in upper atmospheric chlorine, *Geophys.*  
38 *Res. Lett.*, 33, L23813, doi:10.1029/2006GL027600.

- 1 Hocke, K., et al. (2007), Comparison and synergy of stratospheric ozone measurements  
2 by satellite limb sounders and the ground-based microwave radiometer SOMORA,  
3 *Atmos. Chem. Phys. Discuss.*, in press.
- 4 Jackson, D., Assimilation of EOS MLS ozone observations in the Met Office Data  
5 Assimilation System, *Atm. Chem. Phys. Discuss.*, submitted.
- 6 Jarnot, R. F., V. S. Perun, and M. J. Schwartz (2006), Radiometric and Spectral  
7 Performance and Calibration of the GHz Bands of EOS MLS, *IEEE Trans. Geos.*  
8 *Remote Sens.*, 44, 1131-1143.
- 9 Jiang, Y. B., et al. (2007), Validation of Aura Microwave Limb Sounder Ozone by  
10 Ozonesonde and Lidar measurements, *J. Geophys. Res.*, submitted to this Aura  
11 special issue.
- 12 Johnson, D. G., K. W. Jucks, W. A. Traub, and K. V. Chance (1995), Smithsonian  
13 stratospheric far-infrared spectrometer and data reduction system, *J. Geophys. Res.*,  
14 100, 3091.
- 15 Lait, L. R., et al. (2004), Non-coincident inter-instrument comparisons of ozone  
16 measurements using quasi-conservative coordinates, *Atmos. Chem. Phys.*, 4, 2345-  
17 2352.
- 18 Livesey, N. J., et al. (2005), Version 1.5 level 2 data quality and description document,  
19 Tech. Rep. JPL D-32381, Jet Propulsion Laboratory.
- 20 Livesey, N. J. et al. (2006), Retrieval algorithms for the EOS Microwave Limb Sounder  
21 (MLS), *IEEE Trans. Geosci. Remote Sensing*, 44, No. 5, 1144.
- 22 Livesey, N. J., et al. (2007), Validation of Aura Microwave Limb Sounder O<sub>3</sub> and CO  
23 observations in the upper troposphere and lower stratosphere, *J. Geophys. Res.*,  
24 submitted to Aura special issue.
- 25 Lumpe, J. D., et al. (2003), Comparison of POAM III ozone measurements with  
26 correlative aircraft and balloon data during SOLVE, *J. Geophys. Res.*, 108, 8316,  
27 doi:10.1029/2001JD000472.
- 28 Manney, G. L. et al. (2007), Derived meteorological products for solar occultation satellite  
29 datasets and comparisons with Aura MLS data, *J. Geophys. Res.*, submitted to this  
30 Aura special issue.
- 31 McGee, T. J., M. Gross, U. N. Singh, J. J. Butler, and P. Kimvilankani (1995), An  
32 improved stratospheric ozone lidar, *Opt. Eng.*, 20, 955-958.
- 33 Natarajan, M., L. E. Deaver, E. Thompson, and B. Magill (2005), Impact of twilight  
34 gradients on the retrieval of mesospheric ozone from HALOE, *J. Geophys. Res.*,  
35 D13305, doi:10.1029/2004JD005719.
- 36 Nazaryan, H., M. P. McCormick, and J. M. Russell III (2005), New studies of SAGE II  
37 and HALOE ozone profile and long-term change comparisons, *J. Geophys. Res.*,  
38 110, D09305, doi:10.1029/2004JD005425.
- 39 Petropavlovskikh I., L. Froidevaux, R. Shetter, S. Hall, K. Ullmann, and P.K. Bhartia  
40 (2007), In-flight validation of Aura MLS ozone with CAFS partial ozone columns, *J.*  
41 *Geophys. Res.*, submitted to this Aura special issue.

- 1 Piccolo, C., and A. Dudhia (2007), Precision validation of MIPAS-Envisat products,  
2 *Atmos. Chem. Phys. Discuss.*, 7, 911-929.
- 3 Randall, C. E., et al. (2003), Validation of POAM III ozone : Comparisons with  
4 ozonesonde and satellite data, *J. Geophys. Res.*, 108, 4367,  
5 doi:10.1029/2002JD002944.
- 6 Raspollini, P., et al. (2006), MIPAS level 2 operational analysis, *Atmos. Chem. Phys.*, 6,  
7 5605-5630.
- 8 Read, W.G., Z. Shippony, M.J. Schwartz, N.J. Livesey, and W.V. Snyder (2006), "The  
9 clear-sky unpolarized forward model for the EOS Microwave Limb Sounder  
10 (MLS)," *IEEE Trans. Geosci. Remote Sensing* 44, No. 5, 1367-1379.
- 11 Read, W. G. et al. (2007), Aura Microwave Limb Sounder upper tropospheric and lower  
12 stratospheric H<sub>2</sub>O and RHi validation, *J. Geophys. Res.*, this special issue, submitted.
- 13 Rodgers, C. D. (1976), Retrieval of atmospheric temperature and composition from  
14 remote measurements of thermal radiation, *Rev. Geophys. Space Sciences*, 14, 609 -  
15 624.
- 16 Rodgers, C. D., and B. J. Connor (2003), Intercomparison of remote sounding  
17 instruments, *J. Geophys. Res.*, 108, doi:10.1029/2002JD002299.
- 18 Russell, J., et al. (1993), The Halogen Occultation Experiment, *J. Geophys. Res.*, 98,  
19 10,777-10,798.
- 20 Schoeberl, M. R., et al. (2006a), Overview of the EOS Aura mission, Experiment, *IEEE*  
21 *Trans. Geosci. Remote Sensing*, 44, No. 5, 1066-1074.
- 22 Schoeberl, M. R., et al. (2006b), Chemical observations of a polar vortex intrusion, *J.*  
23 *Geophys. Res.*, 111, D20306, doi:10.1029/2006JD007134.
- 24 Schoeberl, M. R., et al. (2007a), QBO and Annual Cycle Variations in Tropical Lower  
25 Stratosphere Trace Gases from HALOE and Aura MLS Observations,  
26 *J. Geophys. Res.*, submitted.
- 27 Schoeberl, M., et al. (2007b), A Trajectory Based Estimate of the Tropospheric Ozone  
28 Column Using the Residual Method, *J. Geophys. Res.*, this special issue, submitted.
- 29 Schwartz, M. J., et al. (2006), W. G. Read, and W. V. Snyder, EOS MLS forward model  
30 polarized radiative transfer for Zeeman-split oxygen lines, *IEEE Trans. Geosci.*  
31 *Remote Sensing*, 44, 1182-1191.
- 32 Schwartz, M. J., et al. (2007), Validation of Aura Microwave Limb Sounder temperature  
33 and geopotential height measurements, *J. Geophys. Res.*, submitted to this Aura  
34 special issue.
- 35 Stajner, I., et al. (2007), Assimilated Ozone from EOS-Aura: Evaluation of the  
36 Tropopause Region and Tropospheric Columns, *J. Geophys. Res.*, submitted to this  
37 Aura special issue.
- 38 Toon, G. C. (1991), The JPL MkIV interferometer, *Opt. Photon. News*, 2, 19-21.
- 39 Walker, K. A., C. E. Randall, C. R. Trepte, C. D. Boone, and P. F. Bernath (2005), Initial  
40 validation comparisons for the Atmospheric Chemistry Experiment (ACE), *Geophys.*  
41 *Res. Lett.*, 32, L16S04, doi:10.1029/2005GL022, 388-391.

- 1 Wang, H.-J., D. M. Cunnold, L. W. Thomason, J. M. Zawodny, and G. E. Bodeker  
2 (2002), Assessment of SAGE version 6.1 ozone data quality, *J. Geophys. Res.*, 33,  
3 L03805, doi:10.1029/2005GL025099.
- 4 Wang, H. J., D. M. Cunnold, C. Trepte, L. W. Thomason, and J. M. Zawodny, SAGE III  
5 solar ozone measurements (2006): Initial results, *Geophys. Res. Lett.*, 33, L03805,  
6 doi:10.1029/2005GL025099.
- 7 Wang, P.-H., et al. (2006), Ozone variability in the midlatitude upper troposphere and  
8 lower stratosphere diagnosed from a monthly SAGE II climatology relative to the  
9 tropopause, *J. Geophys. Res.*, 111, D21304, doi:10.1029/2005JD006108.
- 10 Waters, J. W., et al. (2006), The Earth Observing System Microwave Limb Sounder  
11 (EOS MLS) on the Aura satellite, Experiment, *IEEE Trans. Geosci. Remote Sensing*,  
12 44, No. 5, 1075-1092.
- 13 WMO (World Meteorological Organization) (2003), Scientific assessment of ozone  
14 depletion: 2002, Global ozone research and monitoring project, Report No. 47,  
15 Geneva.
- 16 Wu, D.L., et al. (2007), Aura MLS cloud ice measurements and comparisons with  
17 CloudSat and other correlative data, *J. Geophys. Res.*, this special issue, (to be)  
18 submitted.
- 19 Yang, D., D. M. Cunnold, H.-J. Wang, and L. Froidevaux (2007), Mid-latitude  
20 tropospheric ozone columns derived from Aura OMI and MLS data using the TOR  
21 approach and mapping techniques, *J. Geophys. Res.*, submitted.
- 22 Ziemke, J. R., S. Chandra, B. N. Duncan, L. Froidevaux, P. K. Bhartia, P. F. Levelt, J. W.  
23 Waters (2006), Tropospheric ozone determined from Aura OMI and MLS:  
24 Evaluation of measurements and comparison with the Global Modeling Initiative's  
25 Chemical Transport Model, *J. Geophys. Res.*, 111, D19303,  
26 doi:10.1029/2006JD007089.

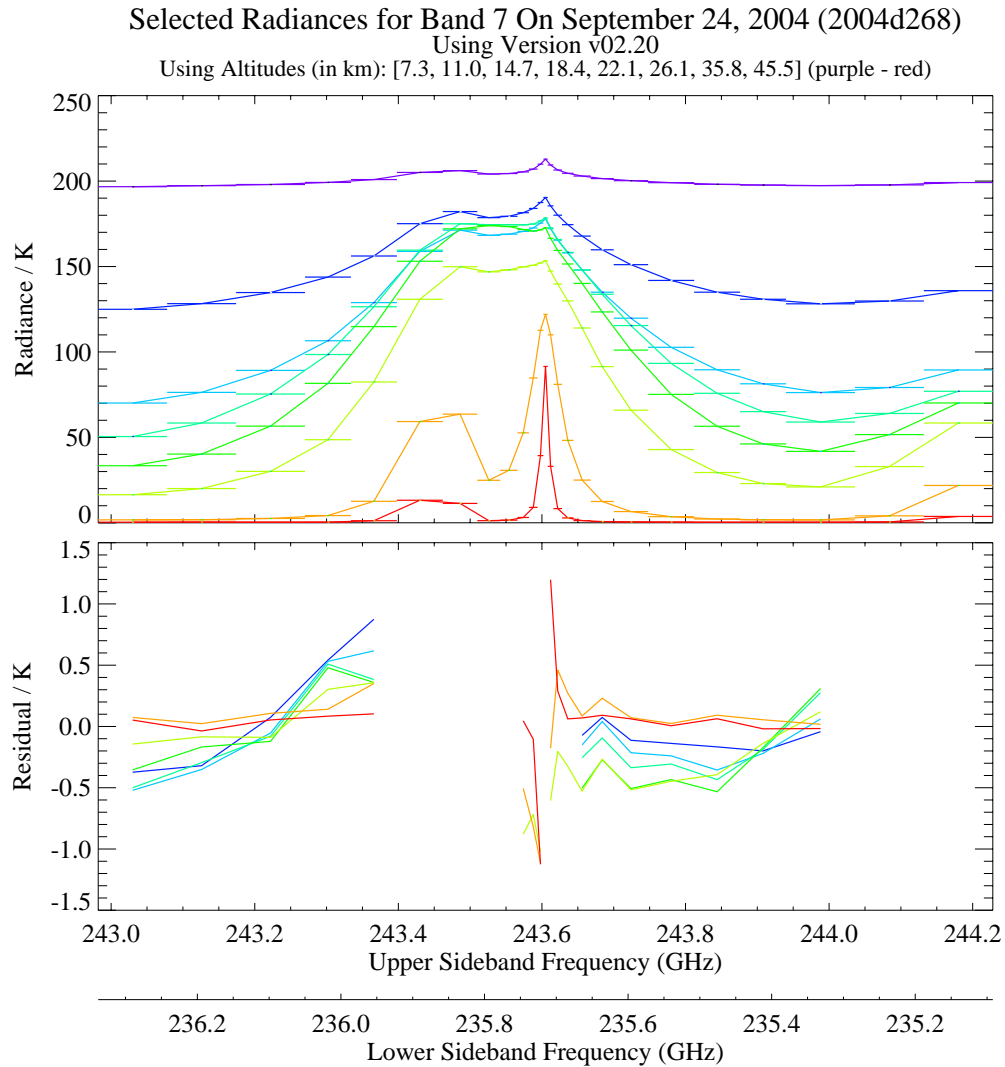


**Figure 1.** Top panel: MLS daily-average radiances for the “band 7” spectral region near 240 GHz, relevant to the retrievals of the MLS standard O<sub>3</sub> product. The primary ozone emission line occurs in the lower sideband and is seen near the center of the plot, with weaker ozone lines (from the upper sideband, folded over in this plot) to the left of it. These radiances are for 24 September, 2004, for average tangent heights of 7 km (purple) to 45 km (red), as indicated above the plot. The x axes provide the frequencies in the upper and lower sidebands, which both contribute to the total radiances measured by MLS. Bottom panel: Residuals (average calculated minus observed radiances) corresponding to each colored curve from the top panel. Channels that are not shown here are not used in the retrievals, except for the very center of the main line, which is covered by fine resolution digital autocorrelator spectrometer (DACS) channels for the mesosphere. Also, optical depth cut-off criteria “turn off” certain channels (near line center) at the lower altitude levels.

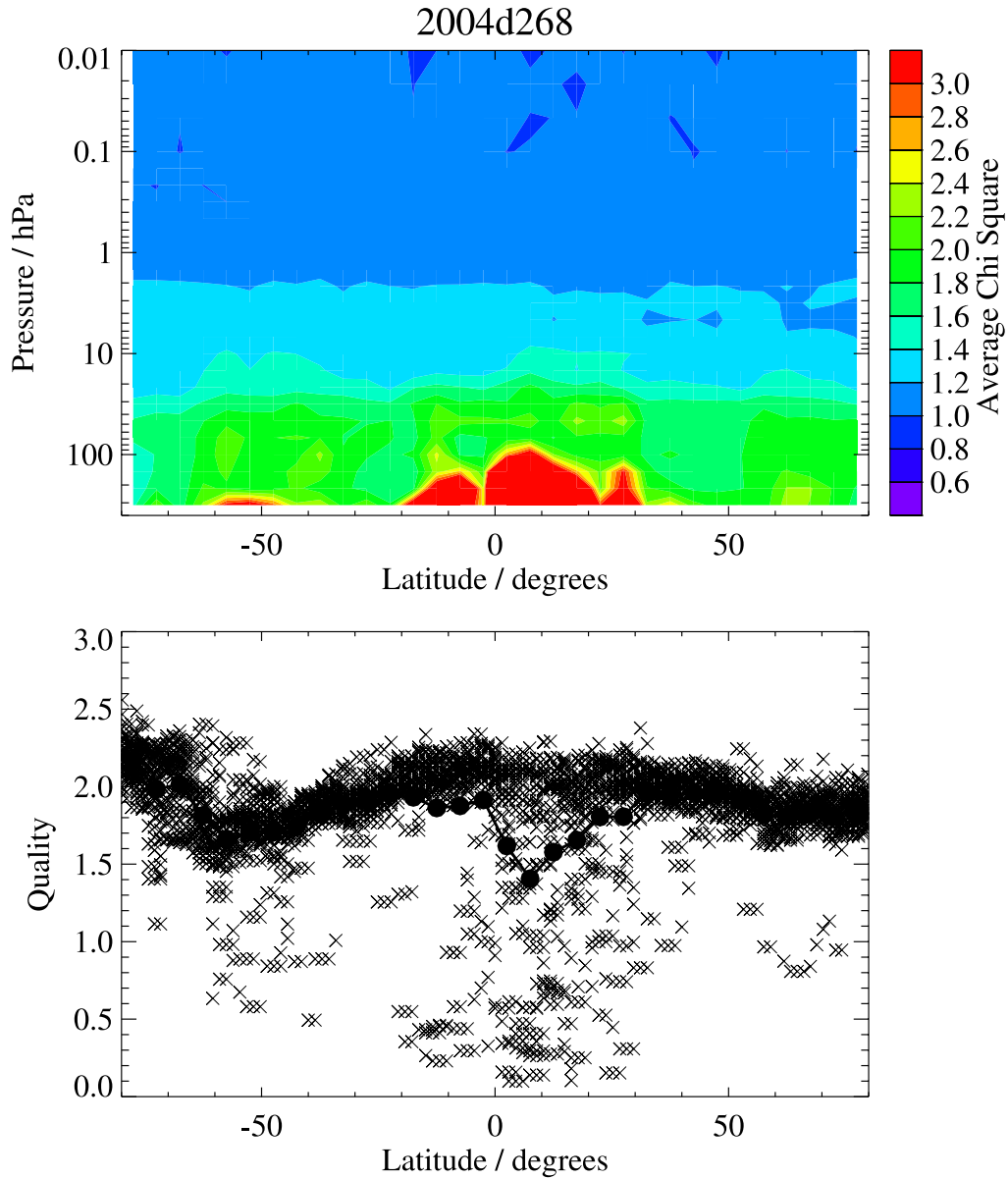


**Figure 2.** Top panel: Zonal mean chi square values (see text) representing the goodness of radiance fits, versus latitude and pressure, for the main MLS ozone band (band 7), on 24 September, 2004. Bottom panel: Values of the related ozone “Quality” field, which is a single number measure of the radiance fits for each profile. Crosses give each “Quality” value versus latitude, and the solid dots joined by a thick line provide zonal mean values.

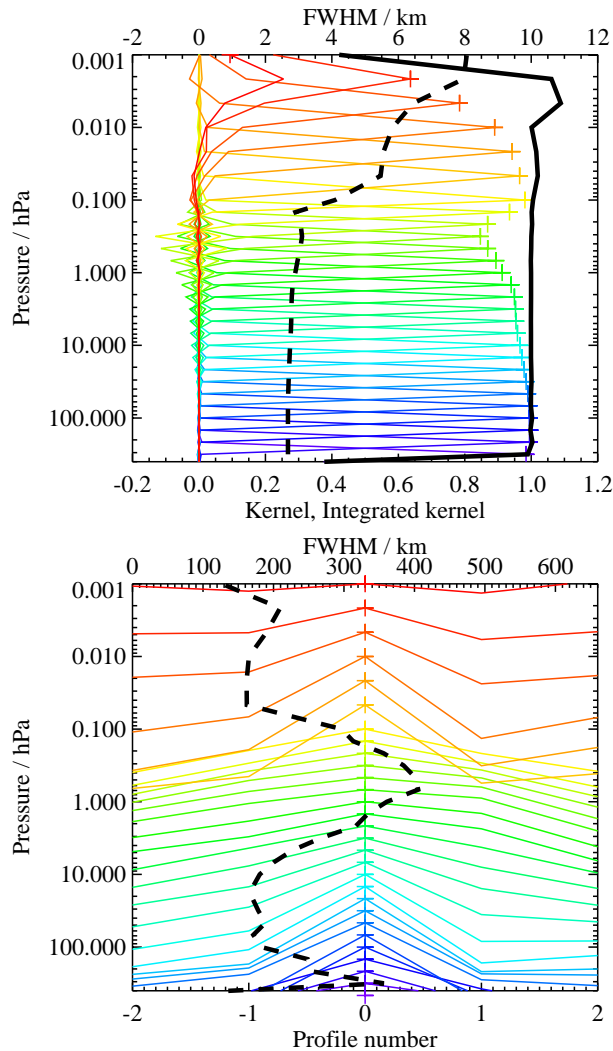


**Figure 3.** Representative averaging kernels (colored lines) and resolution for the v2.2 MLS standard ozone product (from 240 GHz radiances). This example is for 35° N and results for other latitudes are very similar. Top panel: Colored lines show the vertical averaging kernels as a function of the MLS retrieval level, indicating the region of the atmosphere from which information is contributing to the measurements on the individual retrieval surfaces, which are denoted by the plus signs. The kernels are integrated in the horizontal dimension for 5 along-track scans. The dashed black line is the full width at half maximum (FWHM) of these averaging kernels, and indicates the vertical resolution, as given in kilometers above the top axis. The solid black line shows the integrated area under each of the colored curves; a value near unity indicates that most of the information at that level was contributed by the measurements, whereas a lower value implies significant contribution from a priori information. Bottom panel: Colored lines show the horizontal averaging kernels (integrated in the vertical dimension) and dashed black line gives the horizontal resolution, from the FWHM of these averaging kernels (top axis, in km). The averaging kernels are scaled such that a unit change is equivalent to one decade in pressure. Profile numbers along the MLS orbit track are given on bottom axis, with negative values referring to the satellite side of the atmosphere, with respect to the tangent point profile (profile zero); profiles are spaced every 1.5° great circle angle, or about 165 km, along the orbit track.

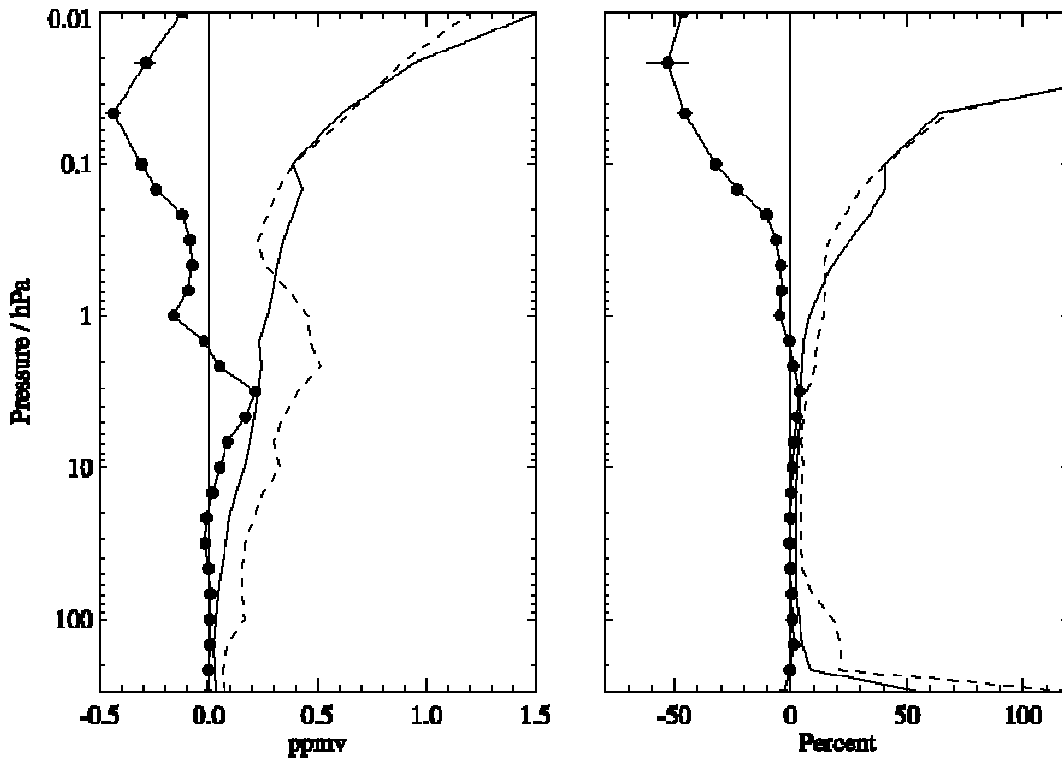


**Figure 4.** The estimated single-profile precision as a function of pressure, for a typical day of MLS data (here, for June 15, 2005), is shown as the solid line (with no dots), based on the root mean square (rms) of MLS retrieval uncertainty estimates (see text), using the 741 matched profile pairs mentioned below. An empirical estimate of precision (repeatability) is given by the dashed line, corresponding to the rms scatter (divided by square root of two) about the mean differences, for all near-coincidences using both ascending and descending MLS profiles (741 matched profile pairs, using a 300 km distance matching criterion). The mean differences are given by the (connected) dots, with error bars (often smaller than the dots) giving the precision (standard error) for these mean differences. Diurnal changes in ozone cause the large mean differences in the mesosphere.

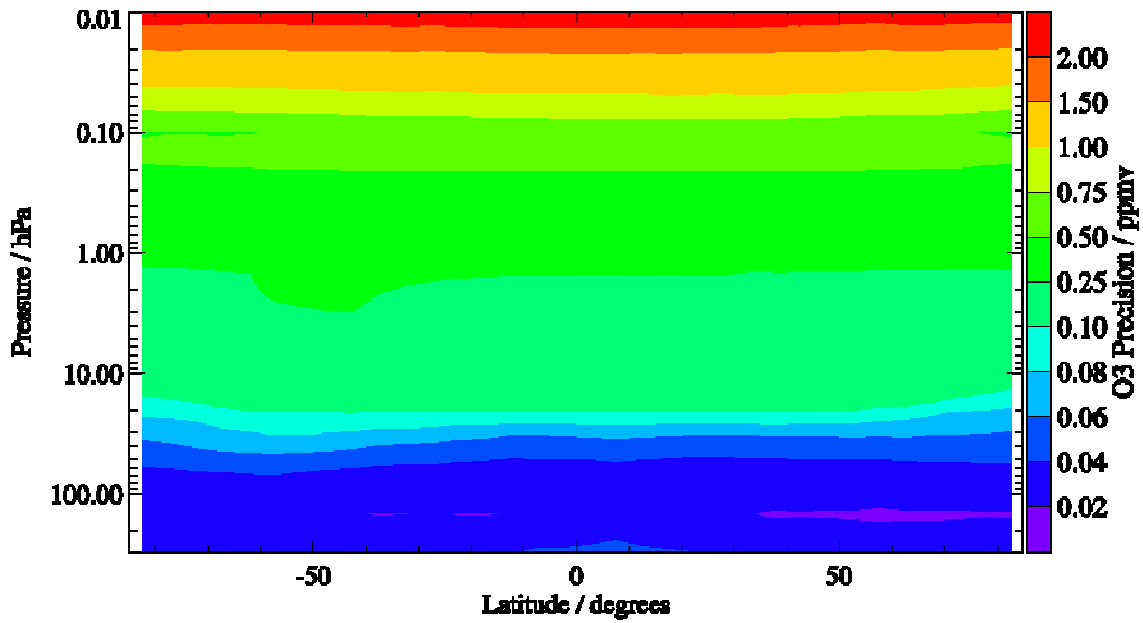


**Figure 5.** Contour plot (pressure versus latitude) of the root mean square precision for MLS ozone profiles on 24 September 2004.

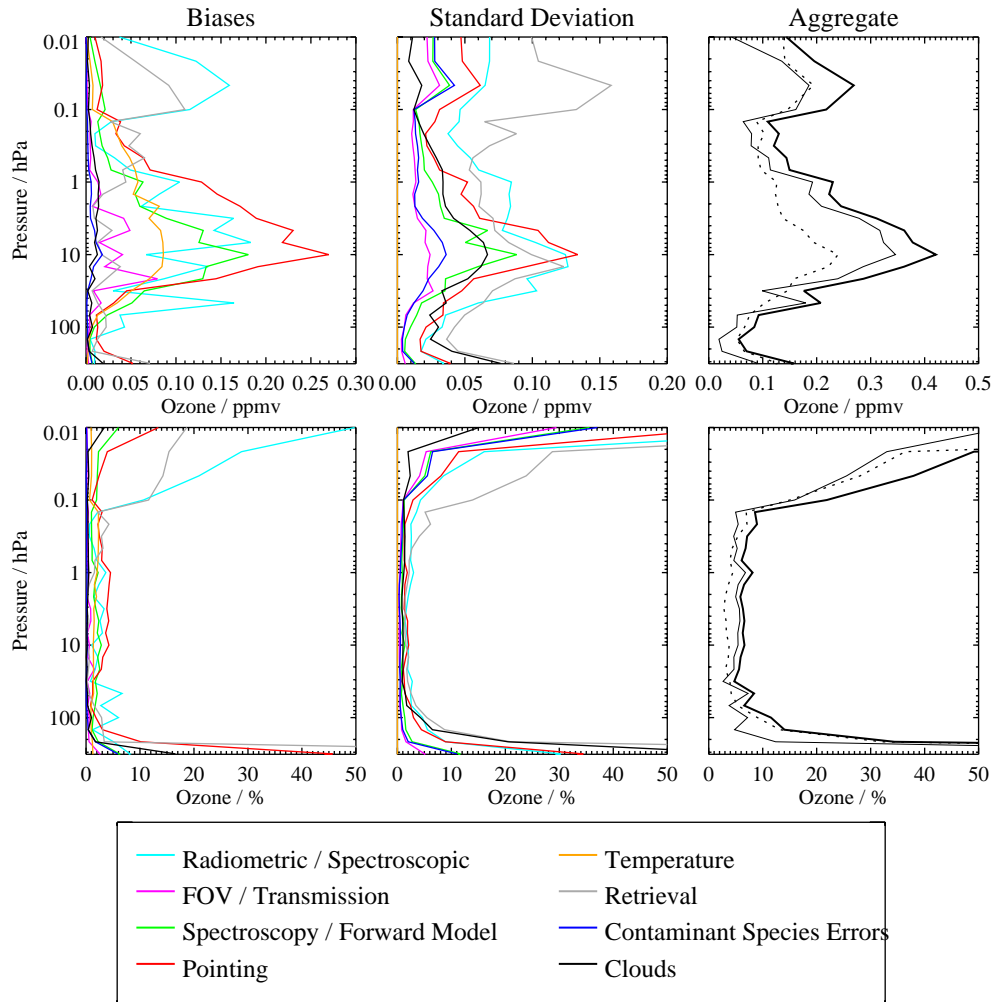


**Figure 6.** Estimated impact of various families of possible systematic errors on the MLS ozone observations. The first two panels show the (left) possible biases and (center) additional rms scatter introduced by the various families of errors, with each family denoted by a different colored line. Cyan lines denote errors in MLS radiometric and spectral calibration. Magenta lines show errors associated with the MLS field of view and antenna transmission efficiency. Red lines depict errors associated with MLS pointing uncertainty. The impact of possible errors in spectroscopic databases and forward model approximations are denoted by the green line, while those associated with retrieval formulation are shown in grey. The gold lines indicate possible errors resulting from errors in the MLS temperature product, while the blue lines show the impact of similar “knock on” errors in other species. Finally, the typical impact of cloud contamination is denoted by the purple line. (Right) the root sum squares (rss) of all the possible biases (thin solid line), all the additional rms scatter (thin dotted line), and the rss of the two (thick solid line).

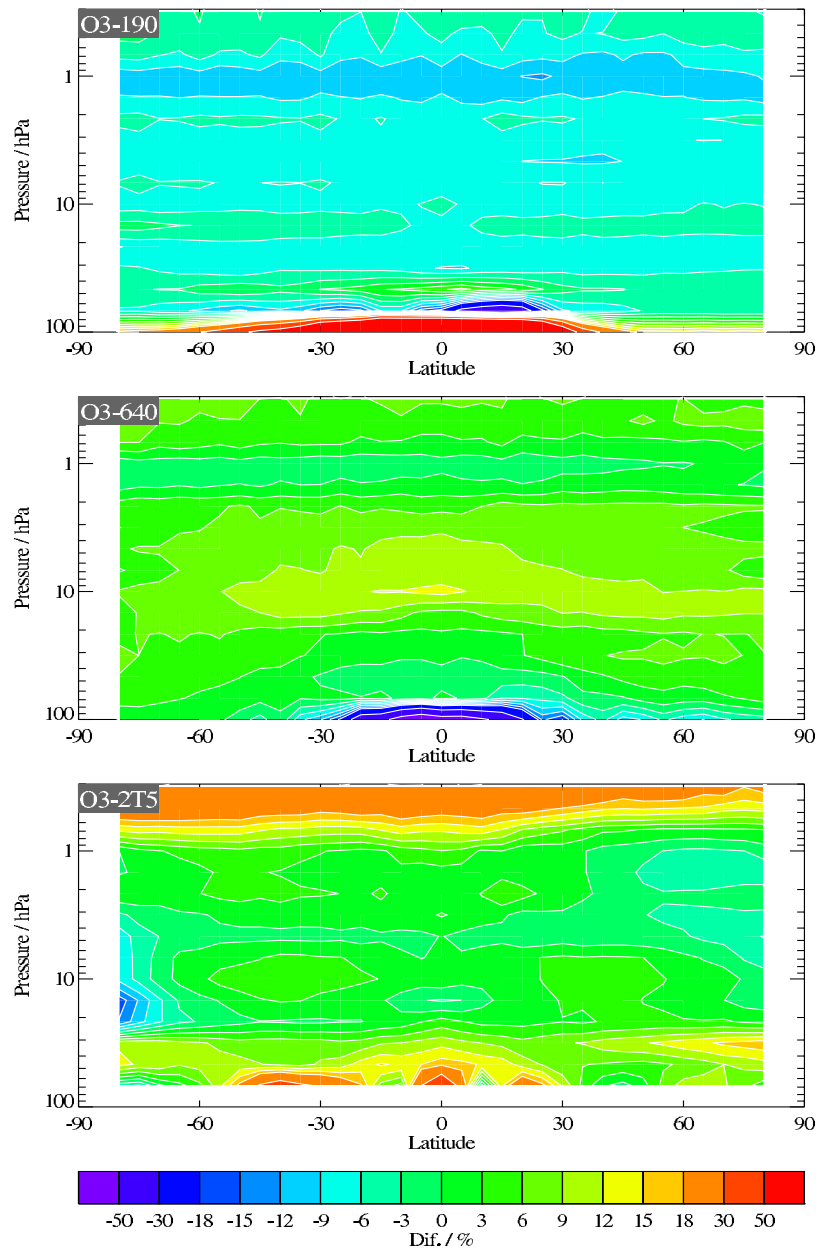


**Figure 7.** Zonal mean differences between retrieved profiles from the MLS 190 GHz (top panel), 640 GHz (middle panel) and 2.5 THz (bottom panel) retrievals and the standard (240 GHz) MLS ozone product. Differences (in percent) are expressed relative to the standard product, positive values meaning larger ozone abundances than the standard, based on averages from 32 days of v2.2 data between 1 February and 31 March, 2005.

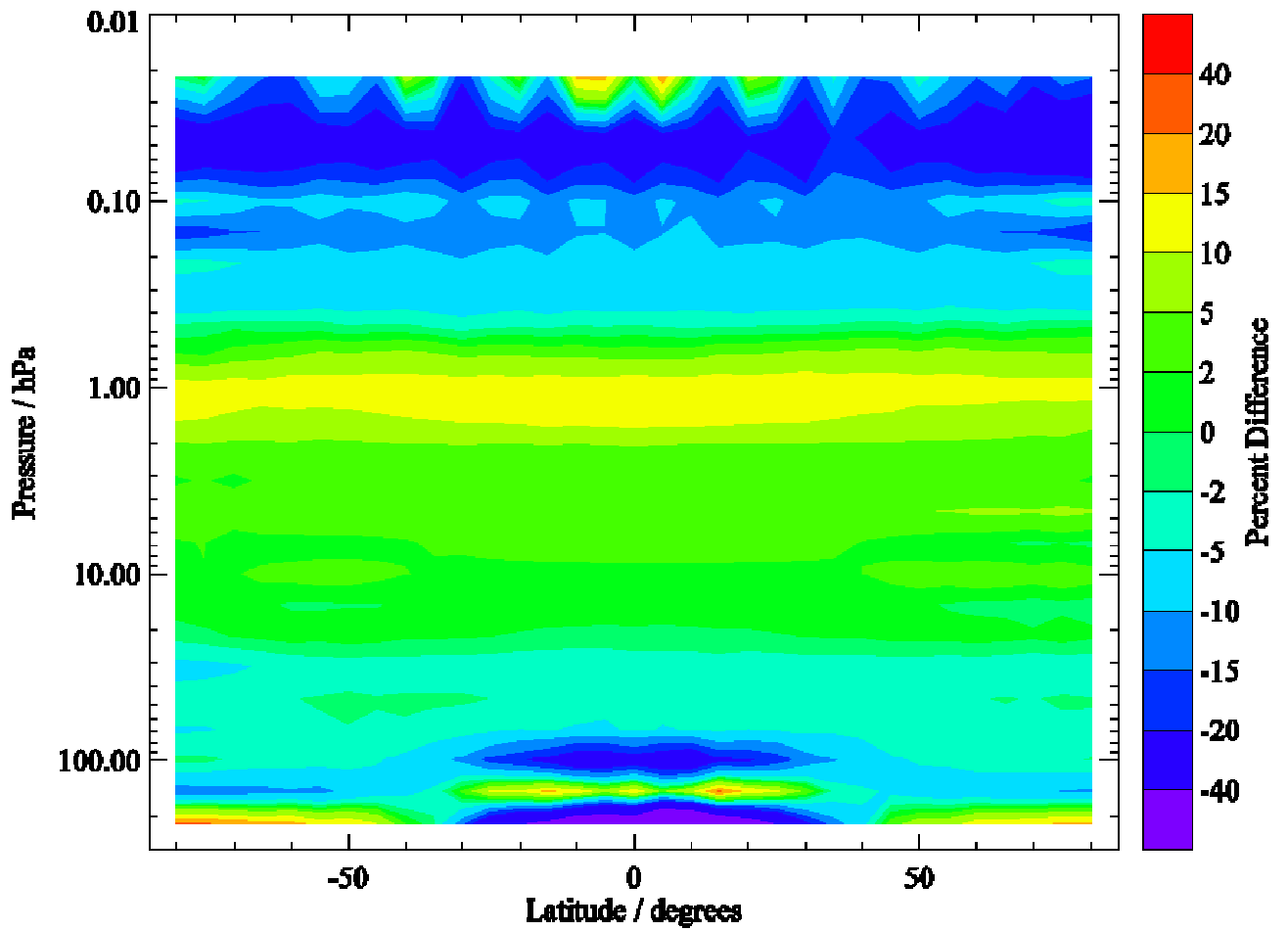


**Figure 8.** Zonal mean difference between MLS ozone abundances from versions 2.2 and 1.5 (v2.2 minus v1.5, expressed as a percentage of v1.5 mean values), based on about 60 days of reprocessed MLS v2.2 data.

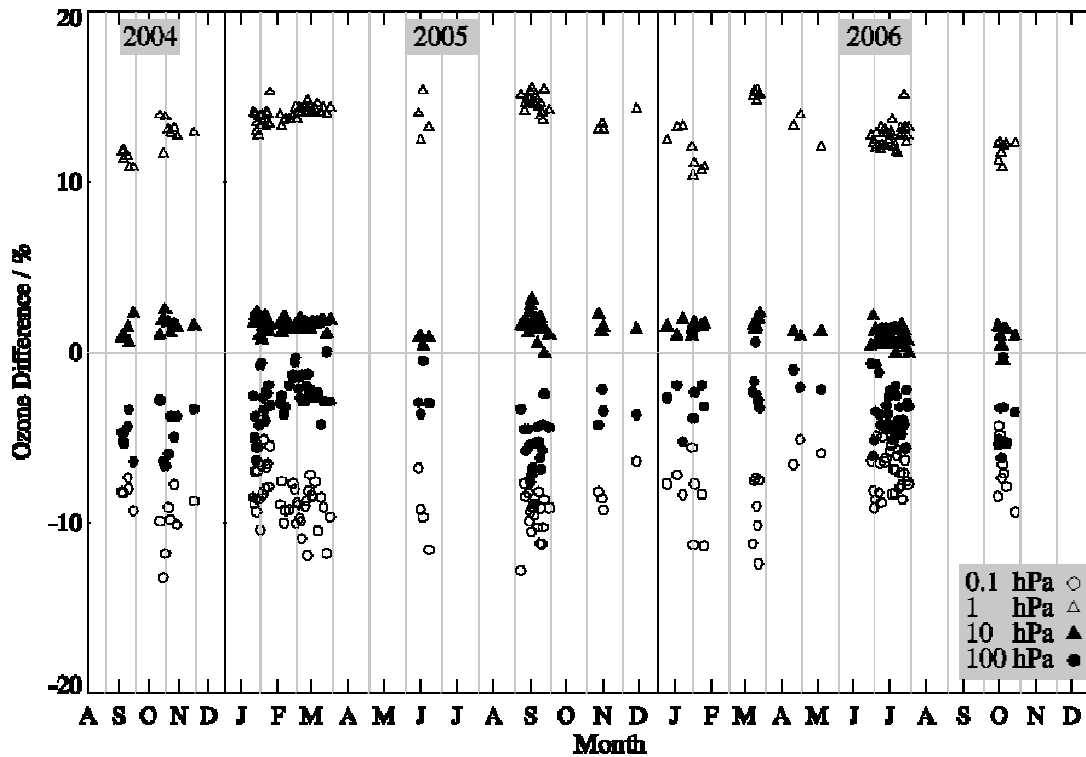


**Figure 9.** Time series of MLS daily global mean ozone differences for v2.2 minus v1.5 data, expressed as a percentage of the v1.5 averages, from available (v2.2) data for late 2004 through 2006. Each symbol type corresponds to a different pressure, as shown in legend at bottom right.

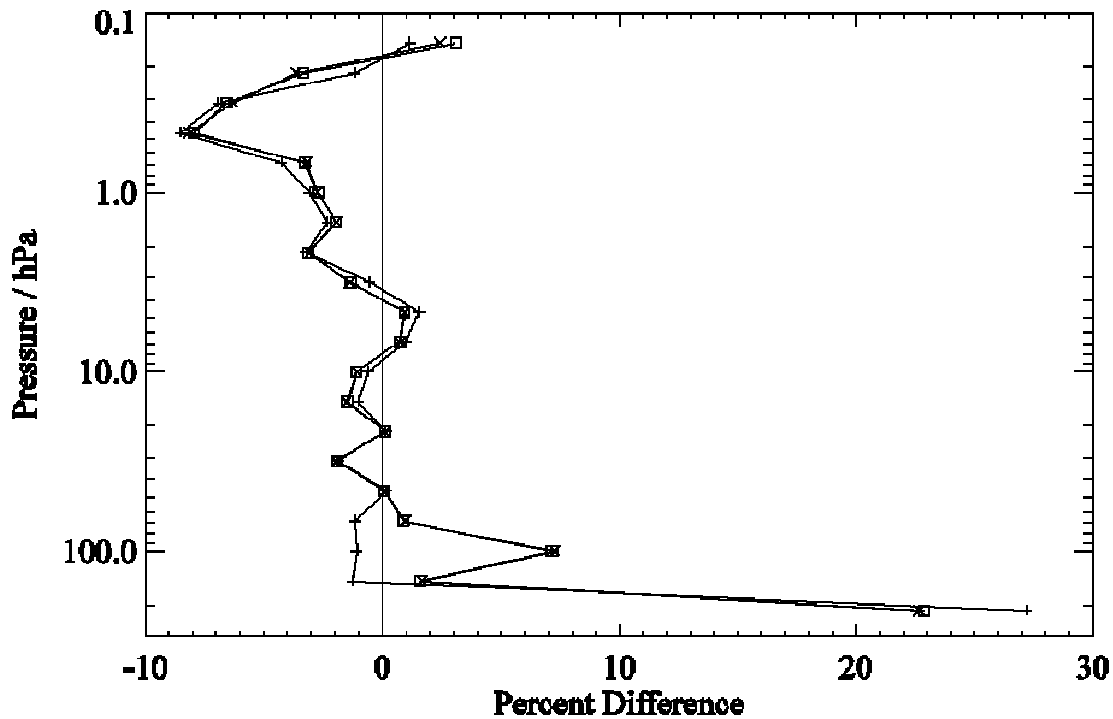


**Figure 10.** Sensitivity of profile differences (v2.2 MLS data minus v6.2 SAGE II data, expressed as a percent of SAGE II averages) to the treatment of SAGE II profiles, coincident with the MLS profiles, for an averaged set of 712 matched profiles from about 50 available days between September 2004 and August 2005. Plus signs represent a simple interpolation method versus log of pressure, crosses are from a least-squares fit of the SAGE II profiles to the MLS retrieval grid, and the open boxes give the result after adding the smoothing effect of the MLS vertical averaging kernels; the latter results are very close to the simpler least-squares formulation, given the generally nicely peaked (and near unity value) of the MLS averaging kernels.

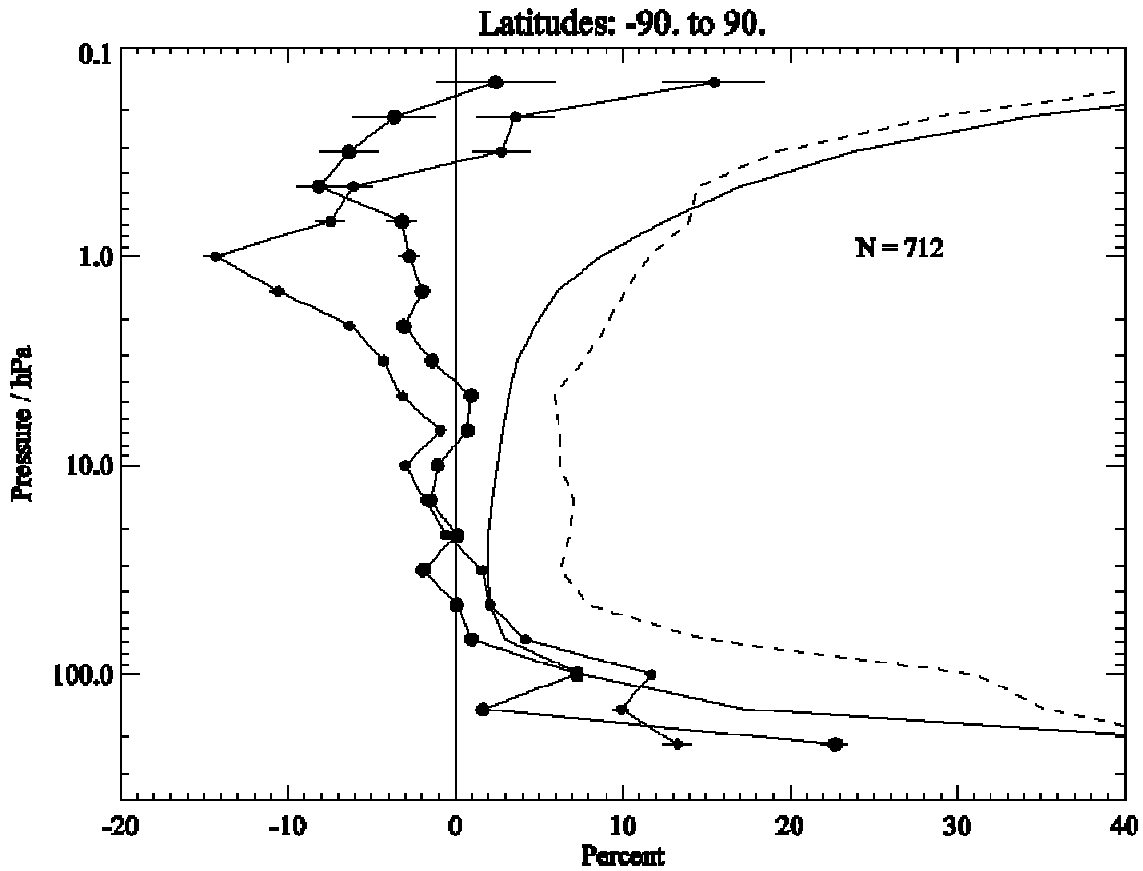


**Figure 11.** Global average differences between MLS and SAGE II ozone profiles, based on coincident profiles obtained from about 50 days of version 2.2 MLS data in 2004 and 2005 (and for 712 matched profile pairs, as indicated by number N above); see text for coincidence criteria used. The large connected dots are for MLS v2.2 data, whereas the small dots are for v1.5 MLS data. Error bars on these dots represent twice the standard error of the mean differences. The dashed curve gives the standard deviation of the differences and the solid curve is an estimate (see text) of the combined precision (random error) of the two measurements.

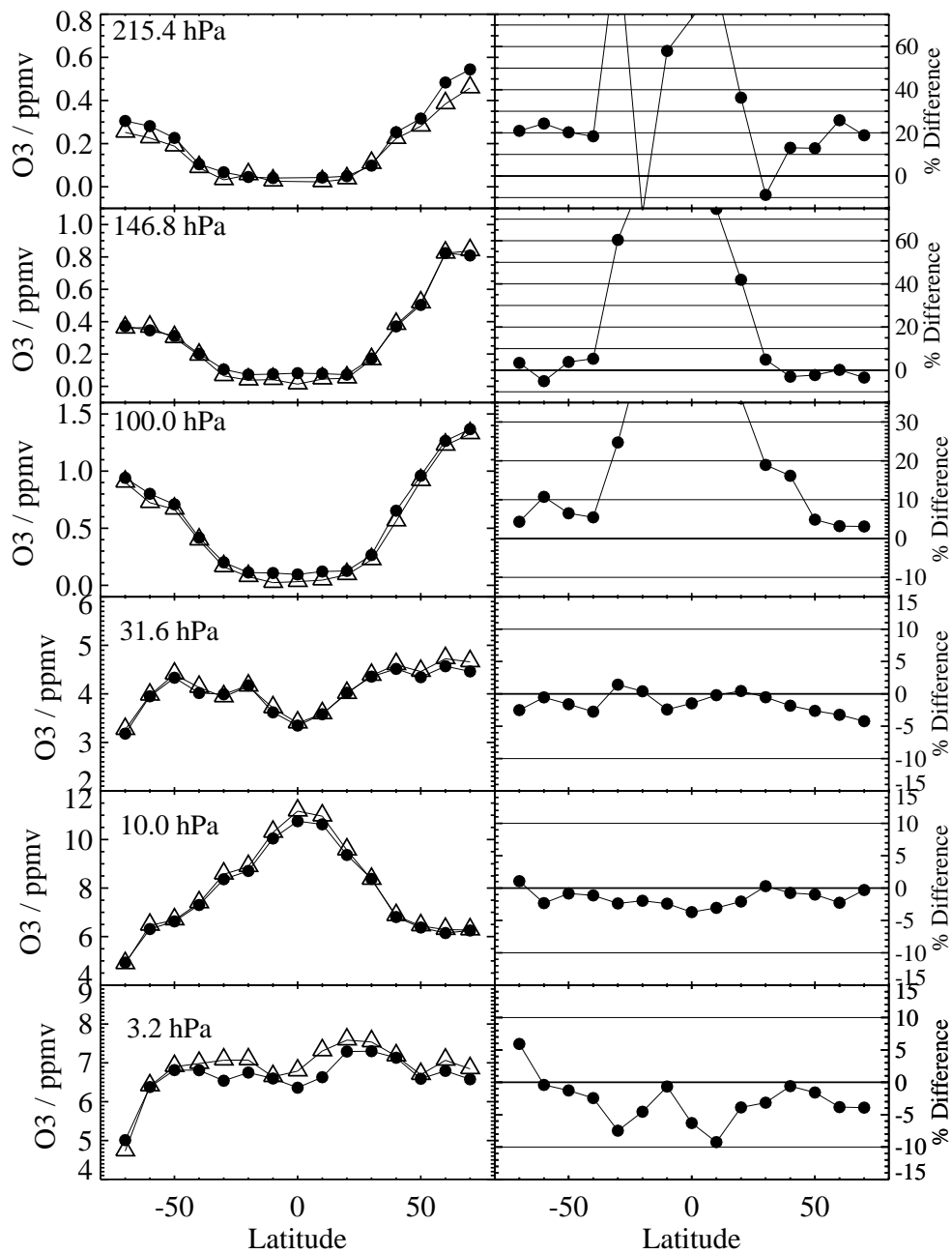


**Figure 12.** Left panels: Zonally-averaged values of ozone versus latitude for coincident measurements from MLS (dots) and SAGE II (triangles) at the pressures indicated in each panel. Right panels: Ozone differences versus latitude for MLS - SAGE II, as a percentage of the mean SAGE II values. The data here apply to all available matched profiles from days reprocessed with MLS v2.2 data, as in Figure 11.

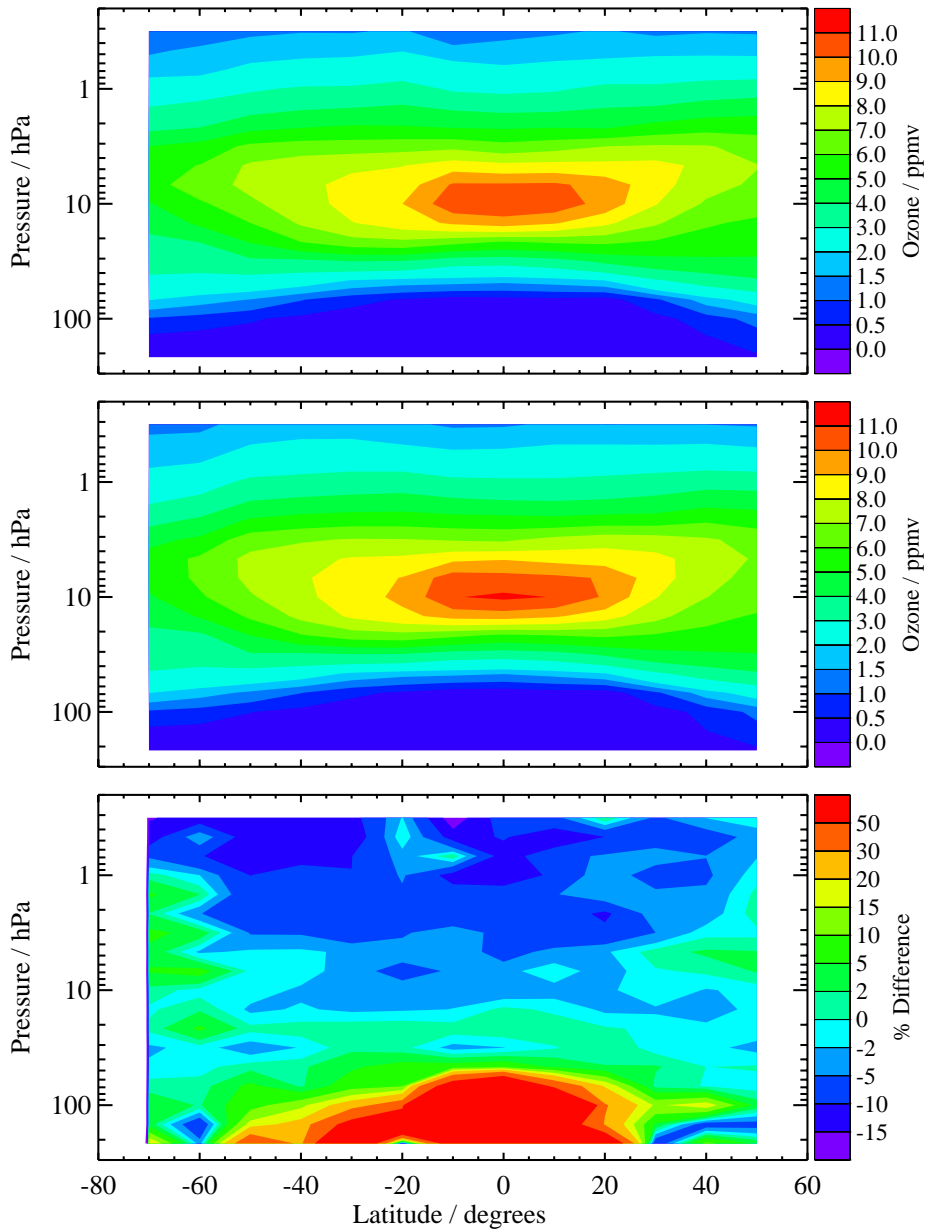


**Figure 13.** Top panel: contour plot of zonally-averaged v2.2 MLS ozone profiles versus latitude for days available from January through March, 2005, including only the coincidences with available SAGE II profiles. Middle panel: the contour plot for SAGE II profiles that are matched to the MLS profiles. Bottom panel: differences MLS - SAGE II, as a percentage of the SAGE II values.

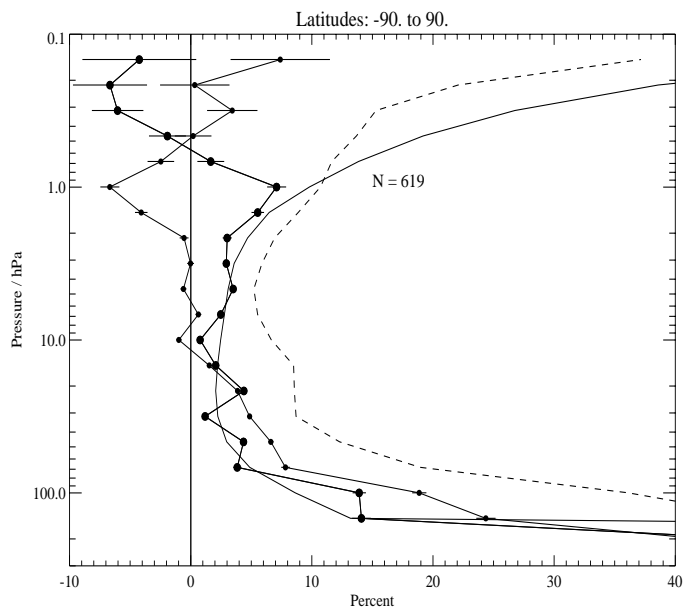
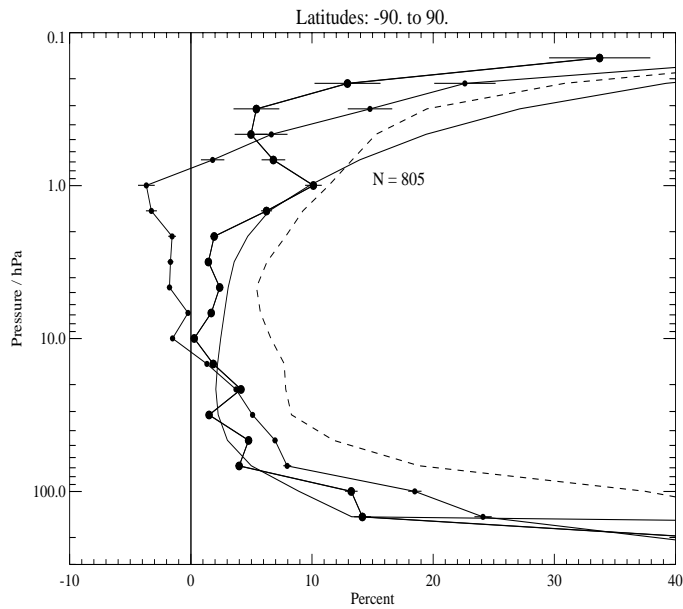


**Figure 14.** Top panel: Same as Figure 11, but for MLS and HALOE (version 19) ozone differences from available 2004 and 2005 matched profile pairs. Bottom panel: Same as top panel, but using MLS daytime observations only.

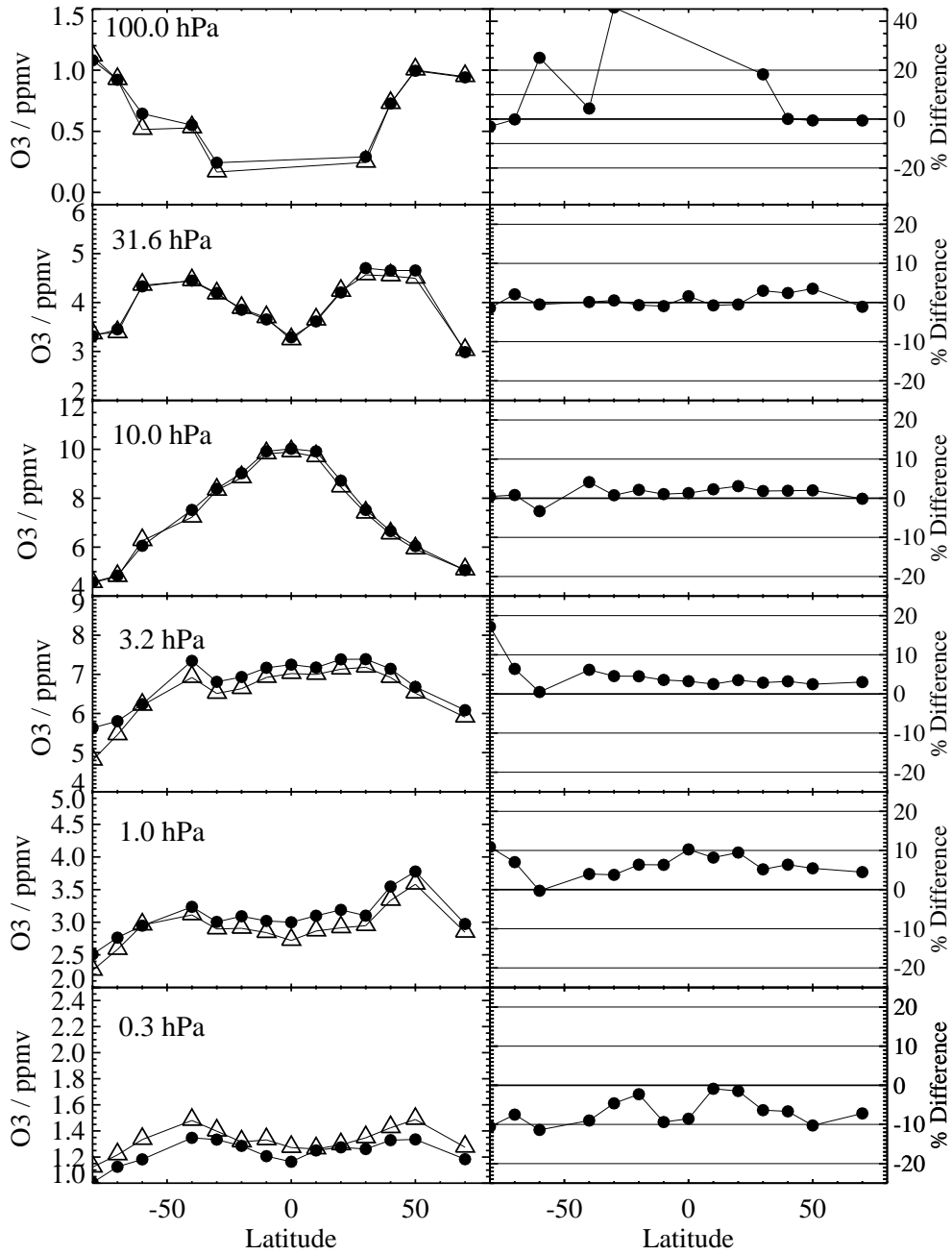


**Figure 15.** Same as Figure 12, but for MLS and HALOE ozone comparisons.

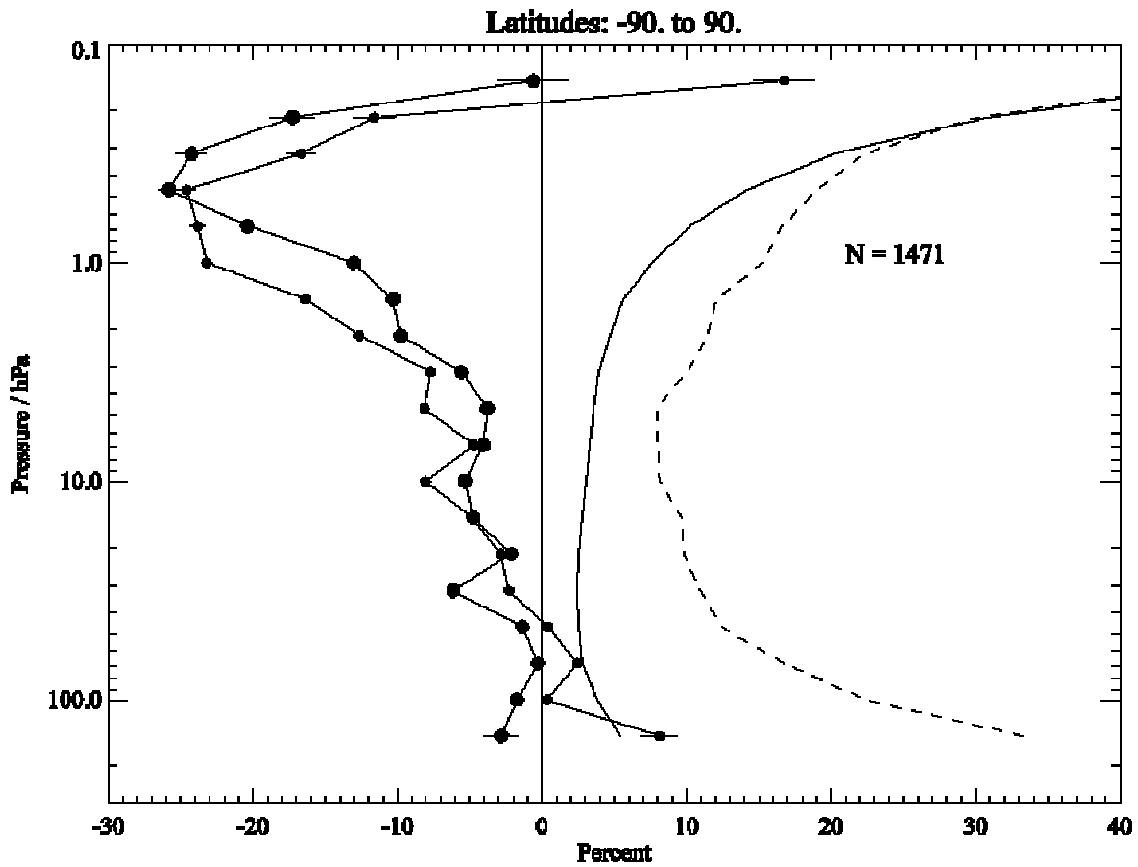


**Figure 16.** Same as Figure 11, but for MLS and ACE-FTS (version 2.2 ozone update) differences (for 1471 available matched profile pairs in 2004, 2005, and 2006).

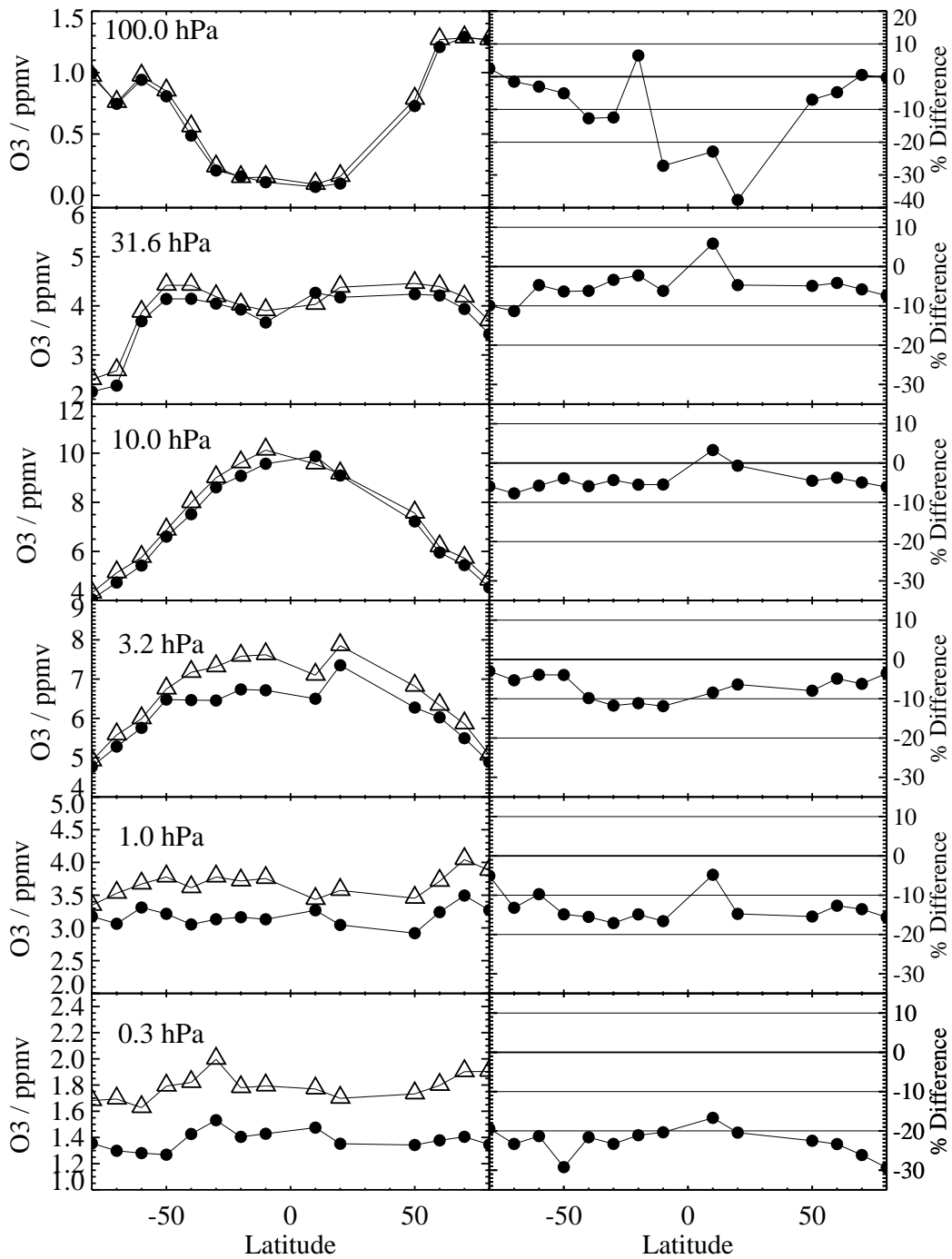


**Figure 17.** Same as Figure 12, but for MLS and ACE-FTS ozone comparisons.

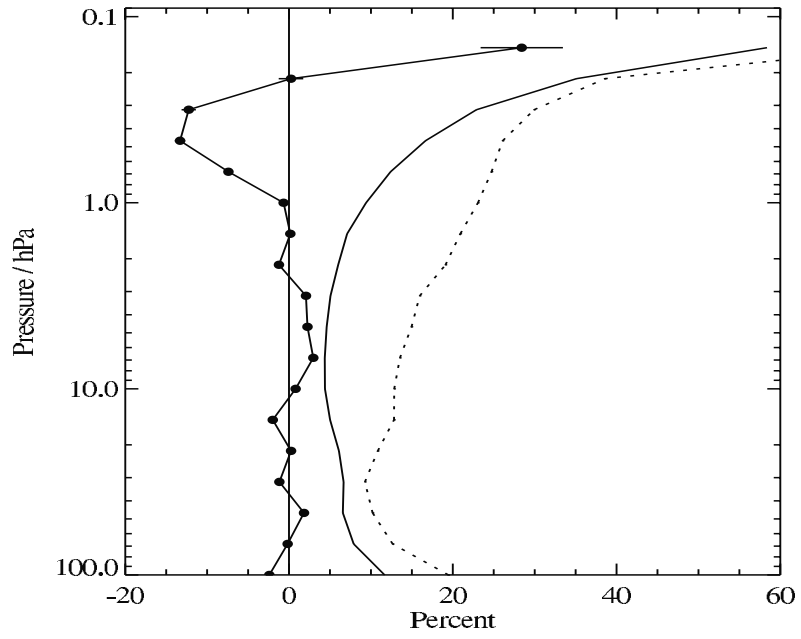


**Figure 18.** Same as Figure 17, but for MLS (version 2.2) and POAM III (version 4) profile comparisons from 2004, 2005, and 2006 (with nearly 700 matched profile pairs).

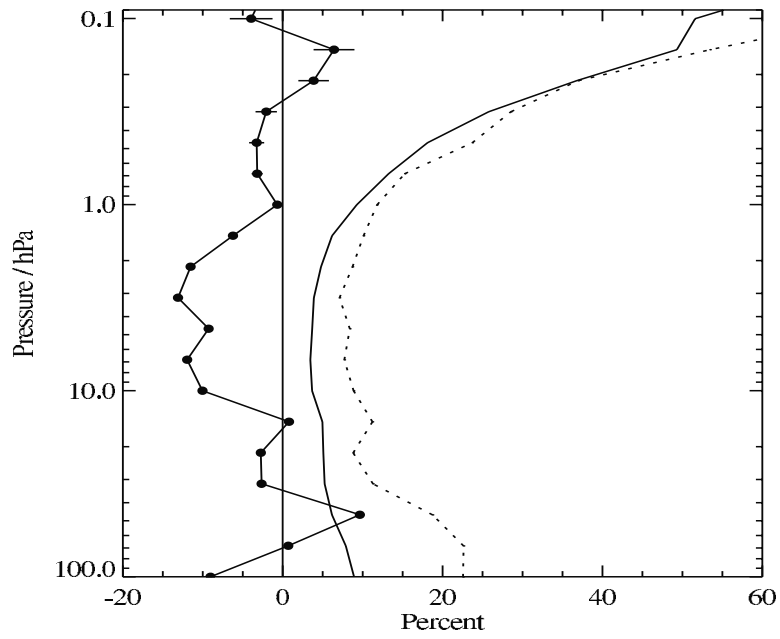


**Figure 19.** Similar to Figure 11, but for differences between MLS (v2.2) and MIPAS (Oxford University retrievals, see text), based on a fraction of one day's comparisons (for 373 profile coincidences), for 28 January, 2005 .

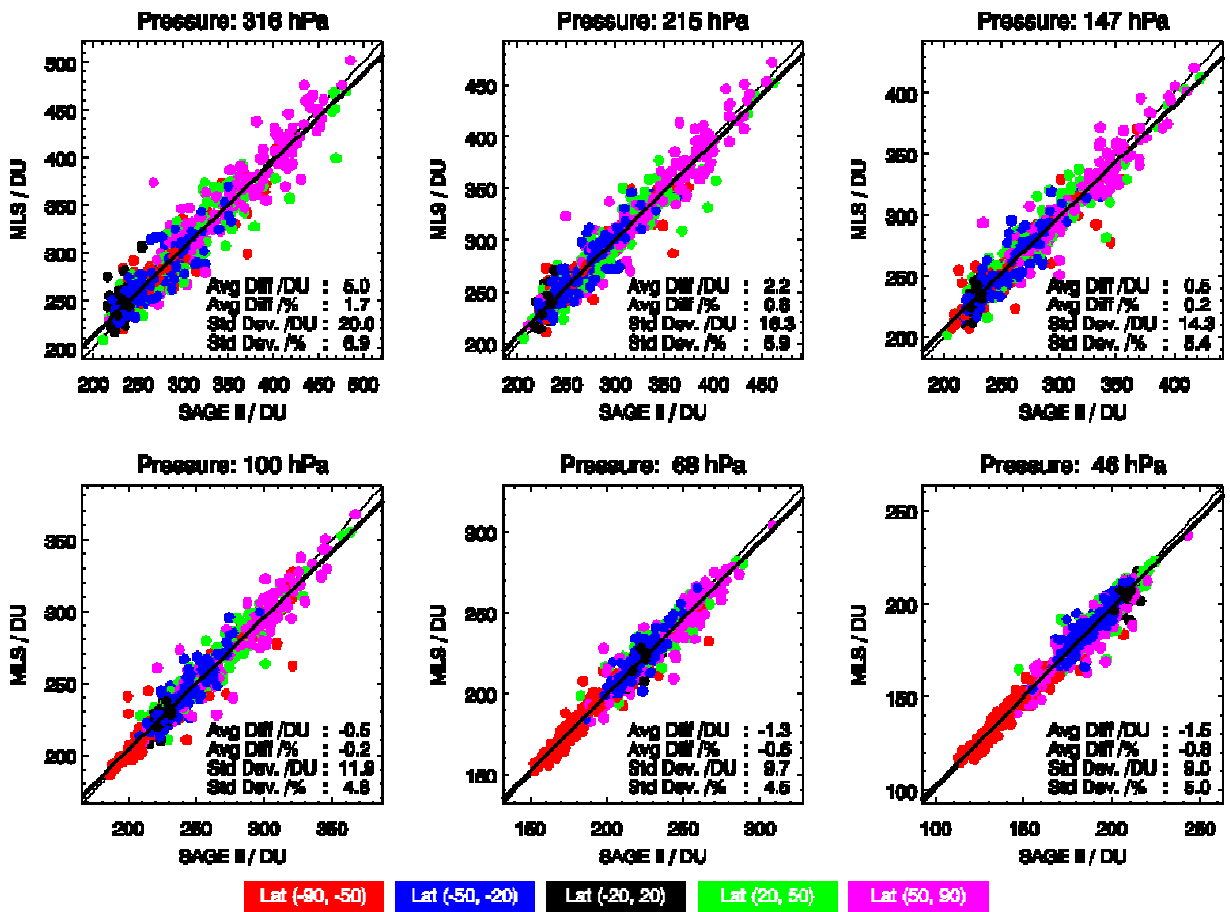


**Figure 20.** Comparison of MLS column abundances versus column ozone values obtained from integrated SAGE II ozone profiles, coincident with the MLS profiles; color coding of points represents different latitude bins, as indicated in the legend. The selected days are based on available days with v2.2 MLS data between August 2004 and August 2005.

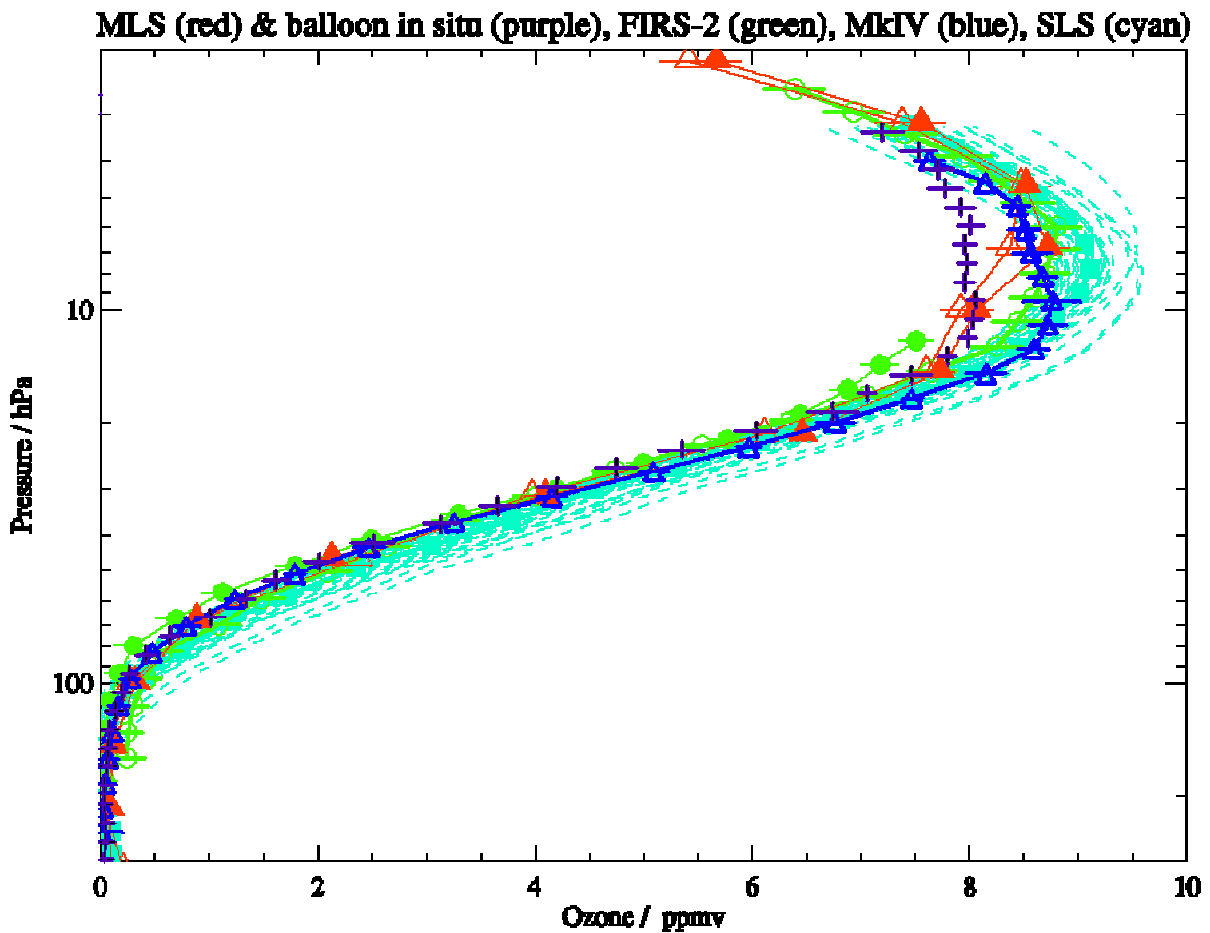


**Figure 21.** Balloon-borne ozone measurements from Ft. Sumner on 20 and 21 September, 2005, in comparison to nearby MLS ozone profiles (v2.2 data), shown as open red triangles for daytime Aura overpass, and closed red triangles for the nighttime overpass. Vertically-averaged values from the fine resolution UV photometer in situ measurements are shown as purple crosses, with variability within each altitude range given by horizontal error bars. FIRS-2 profiles closest in time to the daytime and nighttime MLS overpasses are shown as open and closed green dots, respectively, with precision shown as error bars; the nighttime FIRS-2 profile retrieval is limited to heights below 29 km, where most profile information exists, as the nighttime balloon float altitude dropped below this level. MkIV retrievals (sunset) are shown as open blue triangles with error bars. The SLS profiles (mainly for daytime) are depicted by the relatively close together cyan dashed curves.

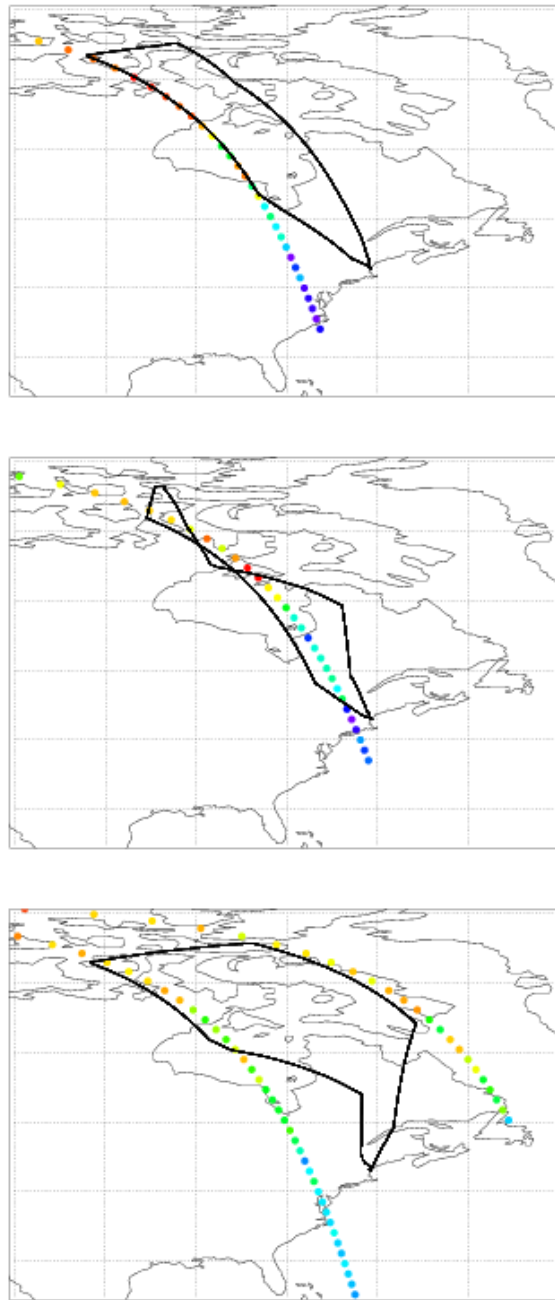


**Figure 22.** Maps depicting the PAVE campaign DC-8 aircraft tracks (solid thick black curves) during three days (top to bottom panels for 27 January, 31 January, and 5 February, 2005, respectively) and superimposed MLS profile locations for coincident satellite sub-orbital tracks shown by colored dots. The dots' color scheme (not shown) corresponds to ozone values at 100 hPa; a more quantitative measure of the compared ozone data from various altitudes is provided in other figures below. The bottom panel results are considered from two close-coincidence legs, the first leg, on the outbound, eastern side, and the second leg on the inbound, western side.

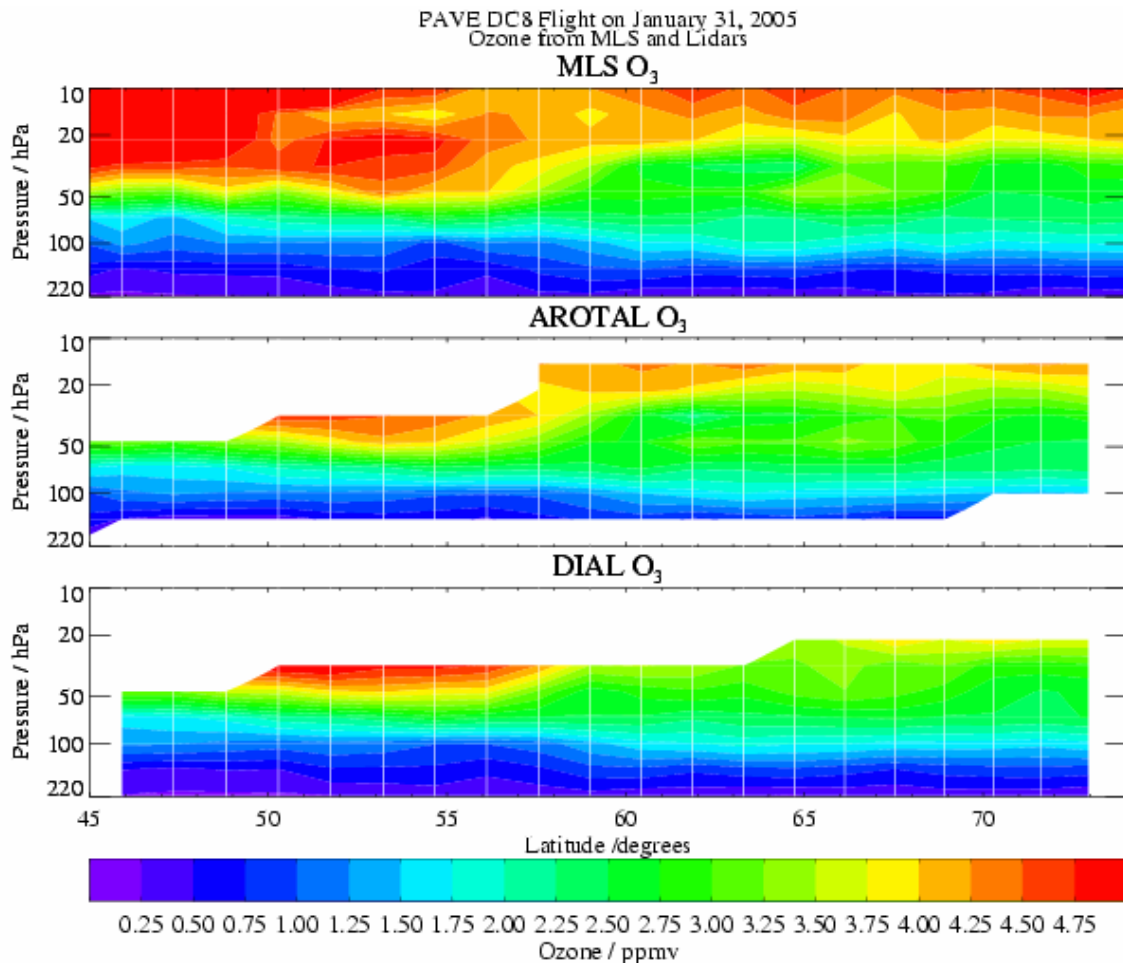


**Figure 23.** Lidar and MLS ozone curtain plots for 31 January, 2005, during the PAVE campaign. MLS, AROTAL, and DIAL retrievals are provided from top to bottom, with the lidar data smoothed to the vertical and horizontal spacing appropriate for MLS (with profile locations indicated by white vertical lines), as discussed in the text.

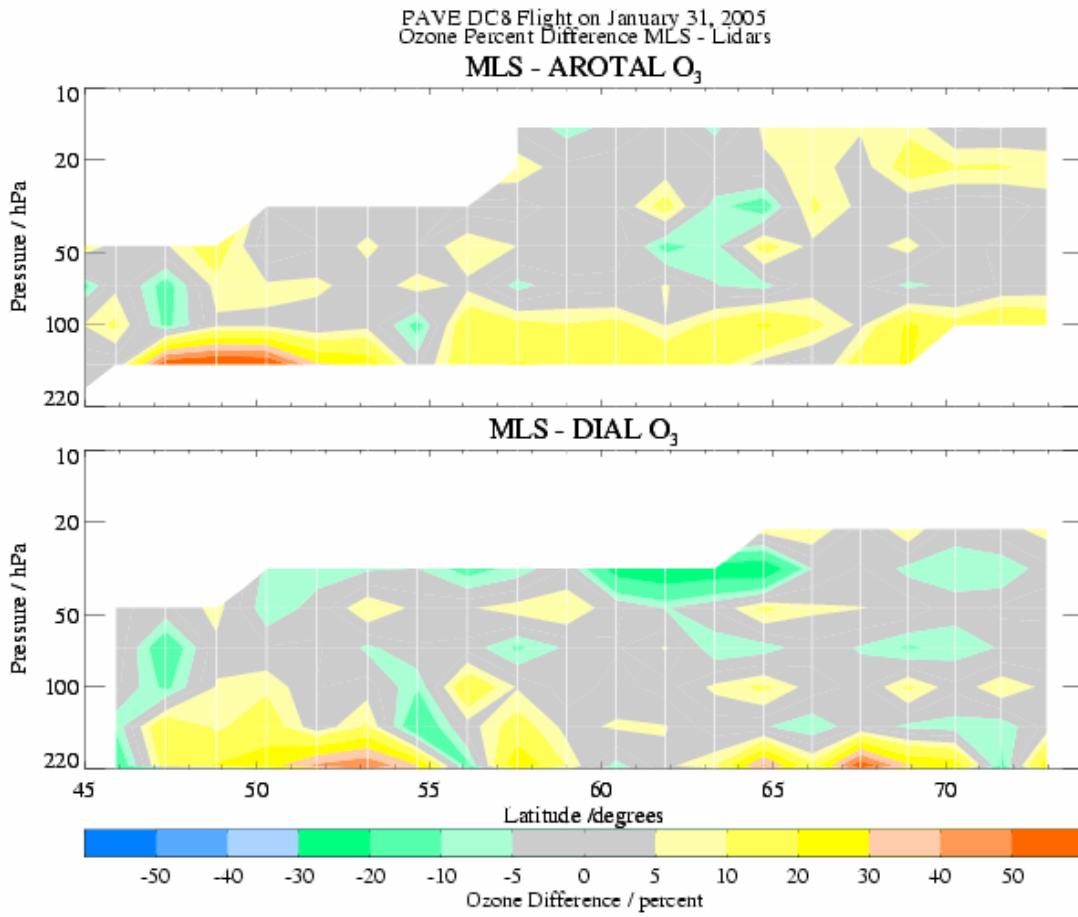


**Figure 24.** Percent differences for MLS ozone minus lidar ozone retrievals, corresponding to the abundances shown in Figure 23.

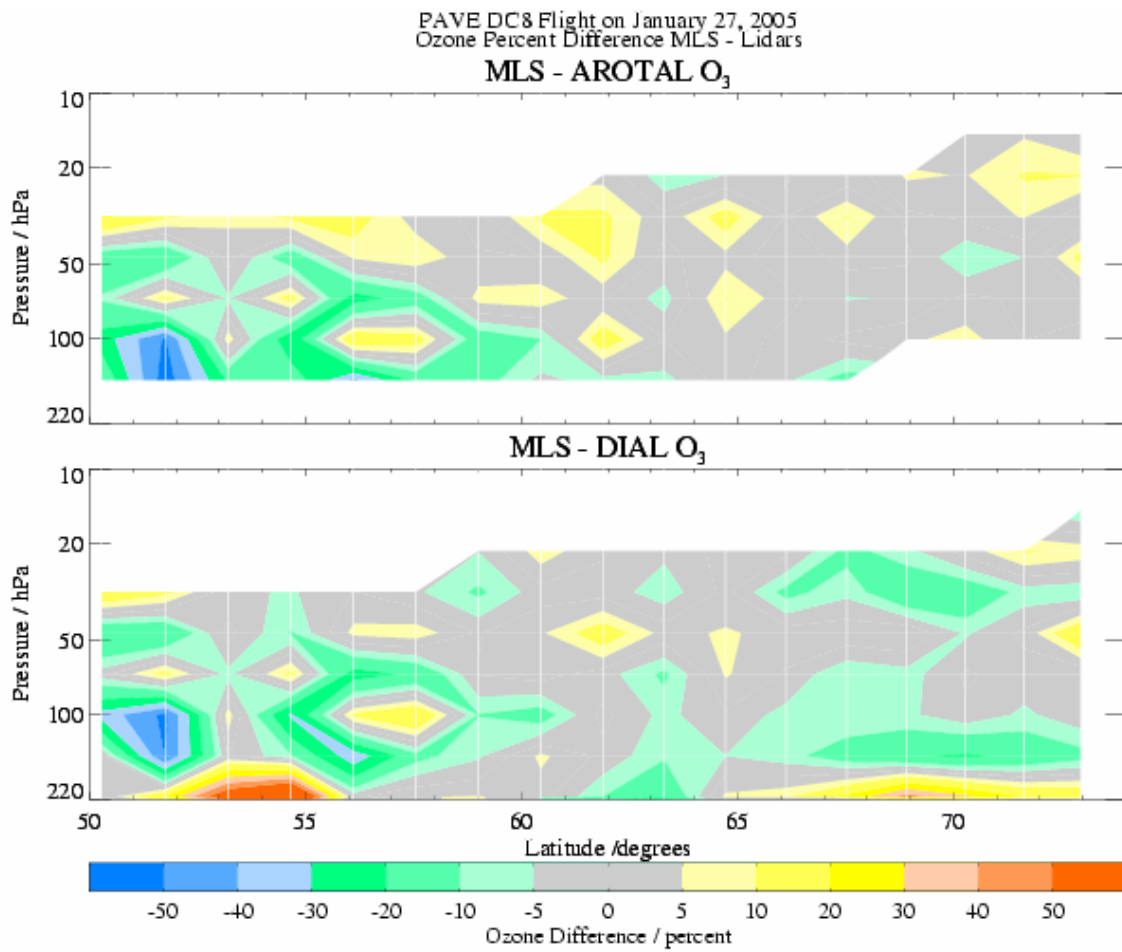


**Figure 25.** Same as Figure 24, except for the PAVE flight and MLS overpass of 27 January, 2005.

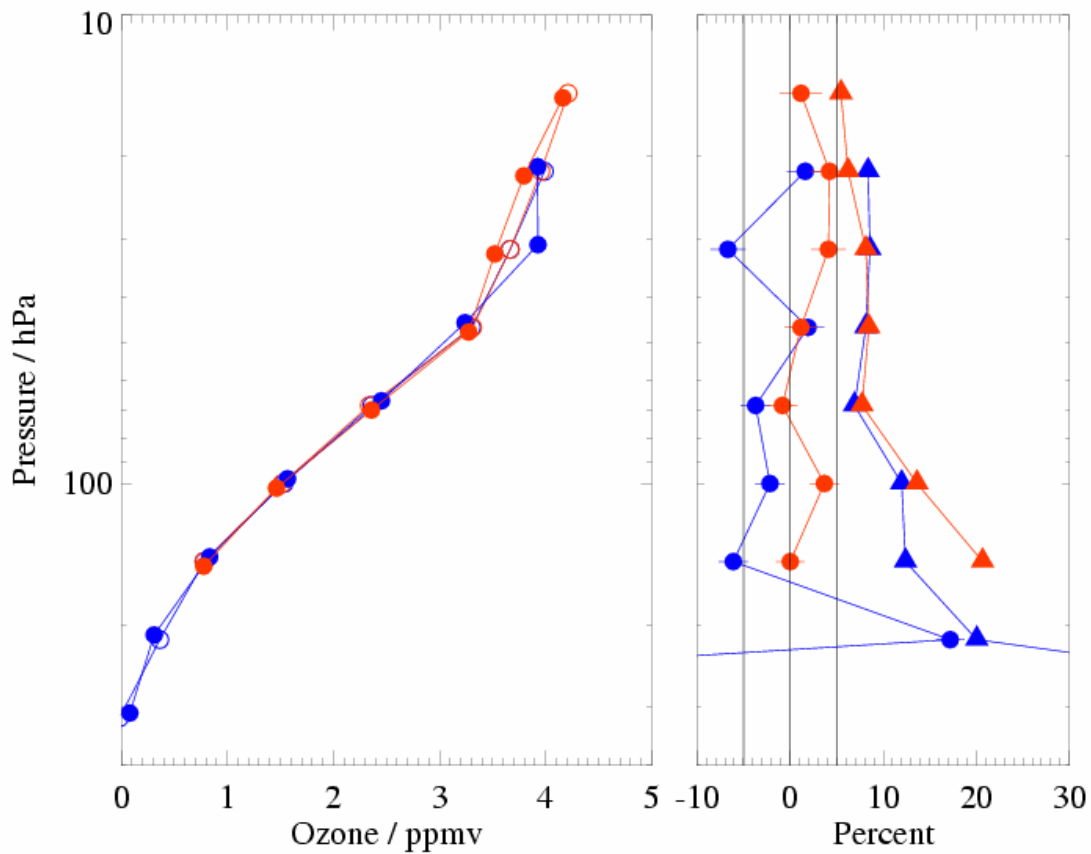


**Figure 26.** Summary of the average MLS and aircraft lidar ozone profiles for the combined set (see text) of coincident DC-8 and MLS measurements during 3 days of the PAVE 2005 campaign, as illustrated in Figure 22. Left panel: average ozone abundances from DIAL (solid blue circles) on the MLS vertical retrieval grid (see text) and from AROTAL (solid red circles) are compared to averages from MLS (open circles, with red and blue values very close to each other, for the averages corresponding to good DIAL and AROTAL data). Right panel: the corresponding percent ozone differences are shown for MLS minus DIAL (solid blue circles) and MLS minus AROTAL (solid red circles), with the standard deviation of the differences shown as triangles of the corresponding colors. Error bars on the average differences represent twice the precision (standard error) in the mean differences. Values at 316 hPa are shown on left panel but not as percent differences (off scale); this level is not generally recommended for MLS ozone data usage.

MLS and AROTAL data for May 1, 2006 (2006d121)

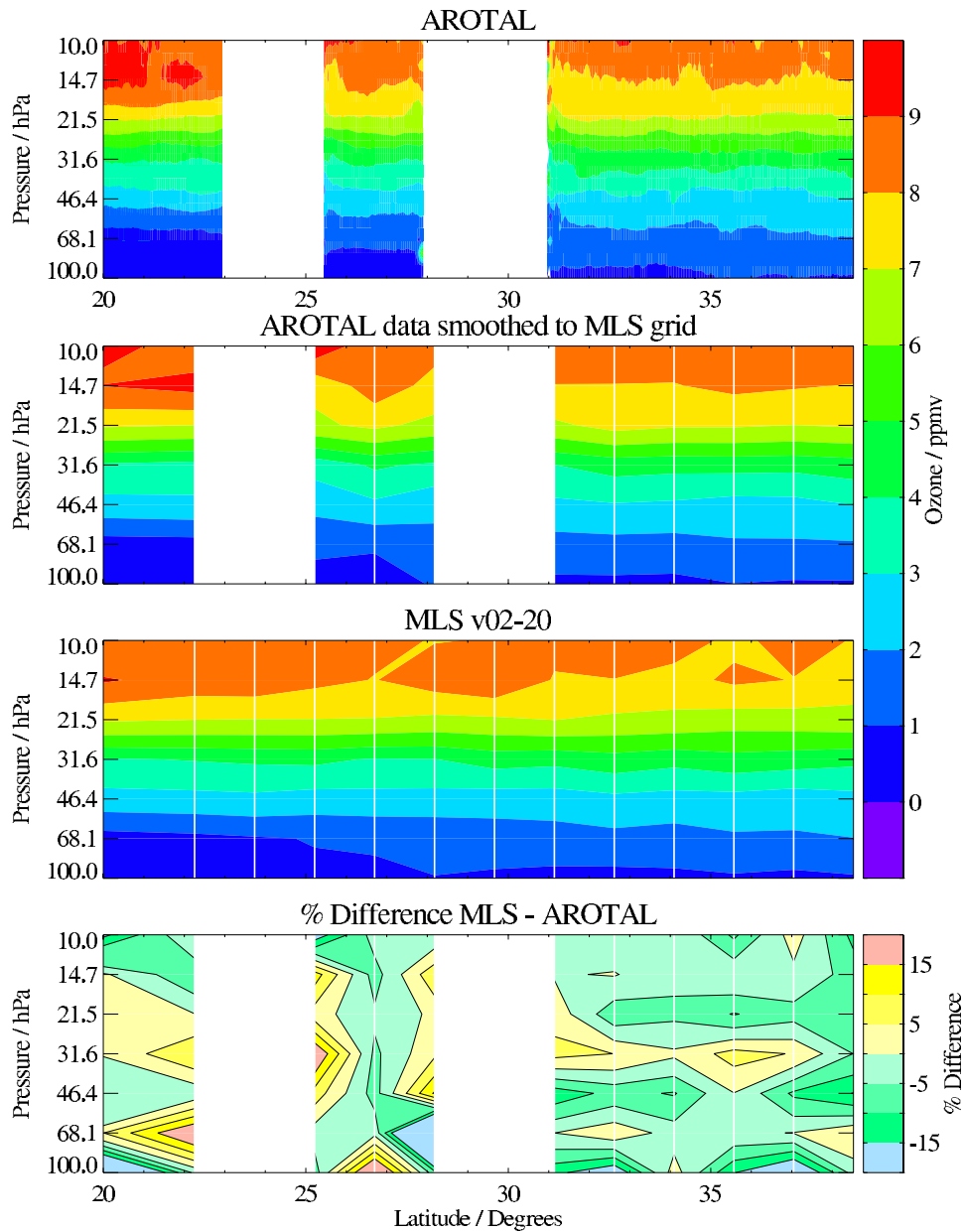


**Figure 27.** INTEX-B lidar ozone data from AROTAL on 1 May, 2006, obtained during the DC-8 transit flight from Hawaii to Alaska, are compared to the MLS ozone profiles at nearby locations (nighttime profiles). From top to bottom, 1st panel shows lidar curtain plot at fine resolution, 2<sup>nd</sup> panel gives the lidar data degraded to the MLS vertical and horizontal grid (see text), 3<sup>rd</sup> panel gives the MLS ozone abundances, and the bottom panel shows the percent difference (MLS minus AROTAL).

MLS and AROTAL data for March 22, 2006 (2006d081)

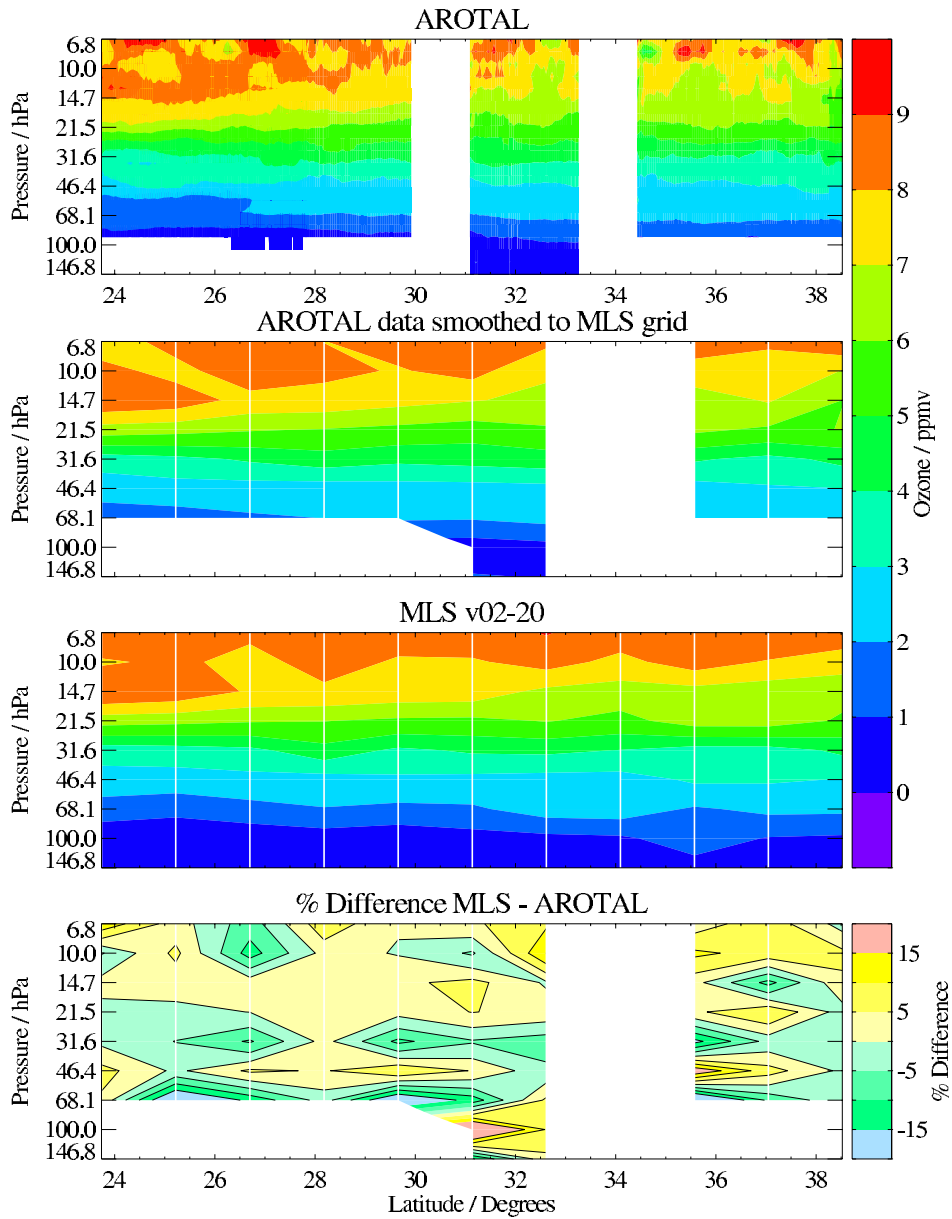


**Figure 28.** Same as Figure 27, but for MLS comparison with INTEX-B AROTAL ozone (lidar) profiles obtained on 22 March, 2006, during the DC-8 transit flight from Houston to NASA Ames.